Article

Cell Host & Microbe

The integrated LIM-peptidase domain of the CSA1-CHS3/DAR4 paired immune receptor detects changes in DA1 peptidase inhibitors in *Arabidopsis*

Graphical abstract

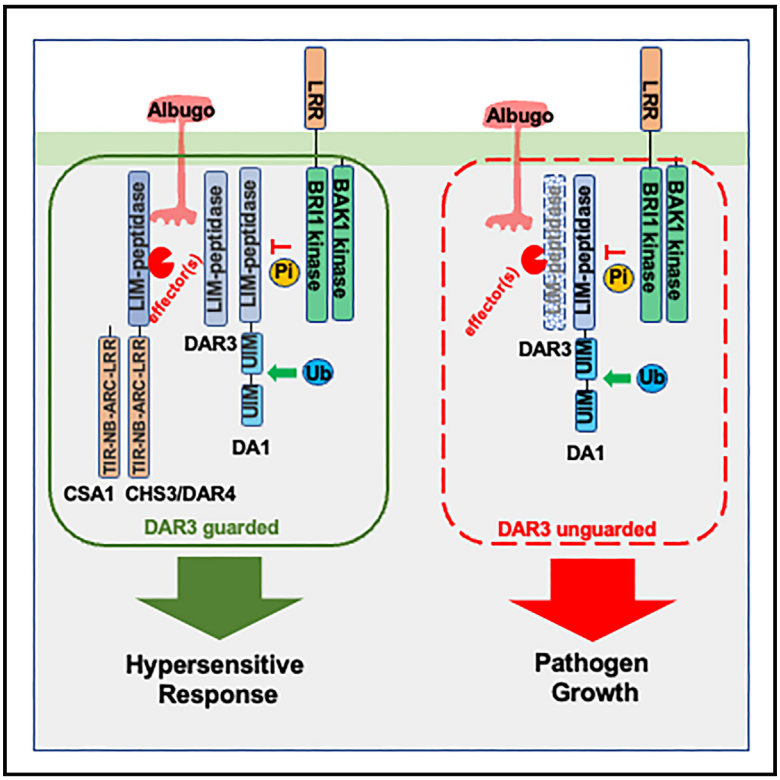

Highlights

- Plant NLR immune receptors integrate domains (IDs) from diverse protein families
- Such IDs detect actions of pathogen effectors and mount defense responses
- Oomycete effectors activate DA1 LIM-peptidases to promote pathogen growth
- LIM-peptidase IDs detect this activation and trigger defense responses

Authors

Benguo Gu, Toby Parkes, Fernando Rabanal, ..., Jonathan D.G. Jones, Volkan Cevik, Michael W. Bevan

Correspondence

jonathan.jones@tsl.ac.uk (J.D.G.J.), volkan.cevik@bath.ac.uk (V.C.), michael.bevan@jic.ac.uk (M.W.B.)

In brief

The DA1 family of LIM-peptidases modulates plant cell proliferation. Gu et al. show that in susceptible hosts, oomycete effectors activate DA1 to facilitate pathogen growth by reducing levels of DAR3, which inhibits DA1. In resistant plants, effector activity is detected by a DAR3-like integrated domain to induce cell death.

Gu et al., 2023, Cell Host & Microbe *31*, 1–13
June 14, 2023
https://doi.org/10.1016/j.chom.2023.04.009

CellPress

Cell Host & Microbe

CellPress
OPEN ACCESS

Article

The integrated LIM-peptidase domain of the CSA1-CHS3/DAR4 paired immune receptor detects changes in DA1 peptidase inhibitors in *Arabidopsis*

Benguo Gu,[1] Toby Parkes,[2,5] Fernando Rabanal,[3] Caroline Smith,[1] Fu-Hao Lu,[1] Neil McKenzie,[1] Hui Dong,[1,6] Detlef Weigel,[3] Jonathan D.G. Jones,[4,*] Volkan Cevik,[2,7,*] and Michael W. Bevan[1,7,*]

[1]Department of Cell and Developmental Biology, John Innes Centre, Norwich Research Park, Norwich NR4 7UH, UK
[2]The Milner Centre for Evolution, Department of Life Sciences, University of Bath, Bath BA2 7AY, UK
[3]Max Planck Institute for Biology Tübingen, Max-Planck-Ring 5, 72076 Tübingen, Germany
[4]The Sainsbury Laboratory, University of East Anglia, Norwich Research Park, Colney Lane, Norwich NR4 7UH, UK
[5]Present address: Rhizocore Technologies Ltd, Roslin Innovation Centre, Edinburgh EH25 9RG, UK
[6]Present address: State Key Laboratory of Crop Genetics and Germplasm Enhancement, Jiangsu Collaborative Innovation Center for Modern Crop Production, Nanjing Agricultural University, Nanjing, China
[7]Lead contact
*Correspondence: jonathan.jones@tsl.ac.uk (J.D.G.J.), volkan.cevik@bath.ac.uk (V.C.), michael.bevan@jic.ac.uk (M.W.B.)
https://doi.org/10.1016/j.chom.2023.04.009

SUMMARY

White blister rust, caused by the oomycete *Albugo candida*, is a widespread disease of Brassica crops. The *Brassica* relative *Arabidopsis thaliana* uses the paired immune receptor complex CSA1-CHS3/DAR4 to resist *Albugo* infection. The CHS3/DAR4 sensor NLR, which functions together with its partner, the helper NLR CSA1, carries an integrated domain (ID) with homology to DA1 peptidases. Using domain swaps with several DA1 homologs, we show that the LIM-peptidase domain of the family member CHS3/DAR4 functions as an integrated decoy for the family member DAR3, which interacts with and inhibits the peptidase activities of the three closely related peptidases DA1, DAR1, and DAR2. *Albugo* infection rapidly lowers DAR3 levels and activates DA1 peptidase activity, thereby promoting endoreduplication of host tissues to support pathogen growth. We propose that the paired immune receptor CSA1-CHS3/DAR4 detects the actions of a putative *Albugo* effector that reduces DAR3 levels, resulting in defense activation.

INTRODUCTION

White blister rust, caused by the oomycete *Albugo candida*, is a widespread disease of Brassica crops including *Brassica juncea* (oilseed mustard) and *B. oleracea*.[1] White rust resistance (*WRR*) genes encoding nucleotide-binding leucine-rich repeat (NLR) immune receptors were identified in oilseed mustard[2,3] and *Arabidopsis thaliana* (*Arabidopsis*).[4,5] Most *Arabidopsis* accessions are resistant to Brassica-infecting *Albugo candida* races.[6] This repertoire of NLR genes can recognize a range of *A. candida* race-specific effectors.[7] Genetic analyses of *Arabidopsis* multi-parent advanced generation inter-cross (MAGIC) lines identified susceptible lines that enabled cloning of multiple *WRR* genes against Brassica-infecting *A. candida* races.[6] This repertoire of NLR genes was proposed to recognize a range of *A. candida* race-specific effectors.

Genetic mapping of Col-5 and Ws-2 *Arabidopsis* recombinant inbred lines (RILs) identified three additional loci that conferred resistance to *A. candida* race AcEM2.[4,5] Of these, the *WRR5* locus contains two resistance genes, *WRR5A* (At5G17880) and *WRR5B* (At5G17890) in a head-to-head configuration. Both *WRR5A* and *WRR5B* are required for conferring chlorotic resistance in transgenic lines of the susceptible accession Ws-2 to *A. candida* AcEM2.[4] Previously, these genes had been identified in mutant screens as *CSA1* (*WRR5A*) and *CHS3* (*WRR5B*).[8] The *chs3-2D* allele causes auto-immune responses requiring *CSA1*, analogous to the requirement of RPS4 for the autoimmunity conferred by its paired partner RRS1^{slh1}, suggesting that CSA1 and CHS3 also form a paired immune receptor.[9] The *chs3-2D* autoimmune allele carries a point mutation in the LIM (Lin-11, Isl-1, and Mec-3)-peptidase (LP) integrated domain (ID) of CHS3/WRR5B: this ID is also found in multiple genomes in the *Brassicaceae*, *Fabaceae*, and *Rosaceae* families.[10,11]

Recent analyses of the natural sequence variation of *CSA1* and *CHS3* in *Arabidopsis* identified three clades, with clade 1 characterized by the LP ID that maintains the CSA1-CHS3 complex in an inactive state. Members of all three clades interact with the BAK1-BIR3 brassinosteroid signaling complex that maintains their inactivity.[5,12] It was proposed that one of the CSA1-CHS3 clades gained an additional defense response specificity through the LP ID while maintaining their guarding

Please cite this article in press as: Gu et al., The integrated LIM-peptidase domain of the CSA1-CHS3/DAR4 paired immune receptor detects changes in DA1 peptidase inhibitors in *Arabidopsis*, Cell Host & Microbe (2023), https://doi.org/10.1016/j.chom.2023.04.009

function toward BAK1-BIR3 integrity.[5] This additional specificity remains uncharacterized.

IDs have been shown to perceive pathogen effectors and their biochemical activities. Analyses of ID functions show they are homologous to proteins that are pathogen-effector targets. When integrated into NLRs, they enable the recognition of effector activities and activation of defense.[9,13–15] They are termed ''integrated decoys'' as they detect effector activities against authentic virulence targets.[11,13,16] Effector molecules produced by pathogens facilitate colonization and reproduction in hosts by subverting cell functions and suppressing innate resistance.[17,18] *Albugo* is an obligate biotroph that infects leaf cells by invaginating the plasma membrane and forming haustoria that take up nutrients produced by living host cells. Multiple aspects of host plant growth and metabolism are modified by effectors that have evolved to support pathogen biotrophic growth. Increasing knowledge of the diverse mechanisms by which effectors modulate plant processes is enabling additional insights into both the regulation of normal host growth and of infection processes.[19,20] Despite exciting progress in understanding ID-effector interactions, the action of most IDs, including the widespread LP IDs, remains poorly understood.

In addition to CHS3, LP domains characterize the eight members of the DA1 family of growth regulators in *Arabidopsis* Col-0.[21] The LIM domain of DA1 comprises two pairs of Zn-finger motifs in a characteristic conformation that confers specificity to protein-protein interactions[22] and a conserved C-terminal Zn metallopeptidase domain with an (A)HEMMH(A) active site.[22,23] The DA1, DAR1, and DAR2 members of the DA1 peptidase family proteolytically cleave and inactivate, via N-end rule mediated proteolysis, diverse proteins involved in cell proliferation to modulate organ size by limiting cell proliferation during organogenesis.[21,23] DA1 peptidases also regulate auxin responses by cleaving transmembrane kinase 1 (TMK1) to release an intracellular kinase domain that relocates to the nucleus to suppress auxin-mediated transcription responses.[24]

The LP ID-containing CHS3 (DAR4) immune receptor carries Toll and interleukin-1 receptor homology region (TIR), leucine-rich repeat (LRR), and nucleotide-binding APAF-1,R proteins and CED-4 (NB-ARC) domains typically found in NLR resistance genes,[21] whereas DAR5 has RPW8 and NB-ARC domains. This suggests that the activities of DA1 family members may be modified by pathogen effectors to support pathogen growth, and these putative immune receptors have evolved to detect this activity.

Gaining a comprehensive understanding of the interplay between pathogens and hosts is key to providing both new insights into the regulation of host plant growth and for predicting pathogenicity and host resistance responses based on genetic and genomic analyses of effector and R gene repertoires.[25,26] Using domain swaps, we show that the LP domain of CHS3/DAR4/WRR5B (referred to henceforth as CHS3/DAR4) is an integrated decoy specifically for the DAR3 member of the DA1 family. *Albugo candida* race AcEm2 induced endoreduplication in infected leaf tissues, and this required DA1 and DAR1 functions, defining them as susceptibility genes. DA1 family peptidase activities are negatively regulated by the formation of complexes with other family members,[27] including DAR3 and DAR7. AcEm2 infection led to the rapid degradation of DAR3, activating DA1 peptidase activity, thereby promoting endoreduplication and pathogen growth.

RESULTS

The LIM-peptidase (LP) domain of DAR4 is a target for an *Albugo* effector

To verify that *CHS3/DAR4* and *CSA1* encode proteins that depend on each other for immune receptor function, the *chs3-1* and *chs3-2d* mutant variants, which confer autoimmunity,[28] were transiently co-expressed with *CSA1* in *Nicotiana tabacum*. Both *chs3* mutants led to hypersensitive responses (HRs) and strong cell death reactions only in the presence of CSA1. Wild-type *CHS3/DAR4* co-expressed with *CSA1* did not trigger HR (Figures 1A–1D and S1A–S1C). To confirm their mutual dependence, *CHS3/DAR4* and *CSA1* constructs were co-expressed with genes encoding another R protein pair, RRS1 and RPS4,[10] and tested for HR in *N. tabacum*. As expected, the non-cognate protein pairs did not cause HR (Figure S1D). These observations confirm that CHS3/DAR4 and CSA1 form a functional NLR protein pair.[5]

The mutation in the *chs3-1* allele removes the C-terminal region containing the peptidase active site, whereas the *chs3-2D* mutation disrupts the fourth zinc finger of the *CHS3/DAR4* LIM domain[21,28] (Figure 1A). Such disruptions in DA1 (through the equivalent C274Y mutation) lead to the loss of DA1 peptidase activity.[23] To test whether the integrity of the peptidase active site in CHS3/DAR4 is required for its regulated immune receptor function, two active site mutations abolishing DA1 peptidase activity were introduced into *CHS3/DAR4*: H1488A and H1492A (*dar4*^{pep}) and E1508I and E1509I (*dar4*^{EEII}) (Figure 1A).[23] These mutant *CHS3/DAR4* genes were co-expressed with *CSA1* in *N. tabacum*. All of these LP mutations caused HR in a *CSA1*-dependent way (Figures 1B–1D and S1), indicating that a functionally intact LP domain in DAR4 is required to maintain the capacity of CHS3/DAR4 for CSA1-dependent defense responses. The LP domain of CHS3/DAR4 therefore acts as a potentially integrated decoy. To test this further, *dar4*$^{aa1\text{-}1037}$ and *dar4*$^{aa1\text{-}1237}$ premature termination truncations of the LP domain and two chimeric proteins that swapped the LP domain with a green fluorescent protein (*dar4-LP*^{GFP}) or glutathione S-transferase (*dar4-LP*^{GST}) were made (Figure 1A) and co-expressed with *CSA1* in *N. tabacum* leaves. None of these deletions or domain swaps caused HR (Figure 1B–1D). Thus, *chs3-1*, *chs3-2d*, *dar4*^{pep}, and *dar4*^{EEII} triggered HR, but the DAR4 premature termination variants without an LP domain did not indicated that the LP domain regulates the immune functions of the R protein pair, CHS3/DAR4 and CSA1. In its native conformation, the LP domain suppresses immune responses, whereas changes to the functional integrity of the LP domain lead to CSA1-dependent HR.

Analyses of genomic data suggested that IDs arise by duplication and recombination of host gene regions that are targets of pathogen effectors.[30] For example, the WRKY ID of RRS1 and its homologous WRKY transcription factor are both acetylated by the bacterial effector PopP2,[9,31] triggering HR through RRS1 and RPS4. If the CHS3/DAR4 LP domain responds to putative pathogen effectors that target related members of the DA1 family, there may be structural and functional conservation

Please cite this article in press as: Gu et al., The integrated LIM-peptidase domain of the CSA1-CHS3/DAR4 paired immune receptor detects changes in DA1 peptidase inhibitors in *Arabidopsis*, Cell Host & Microbe (2023), https://doi.org/10.1016/j.chom.2023.04.009

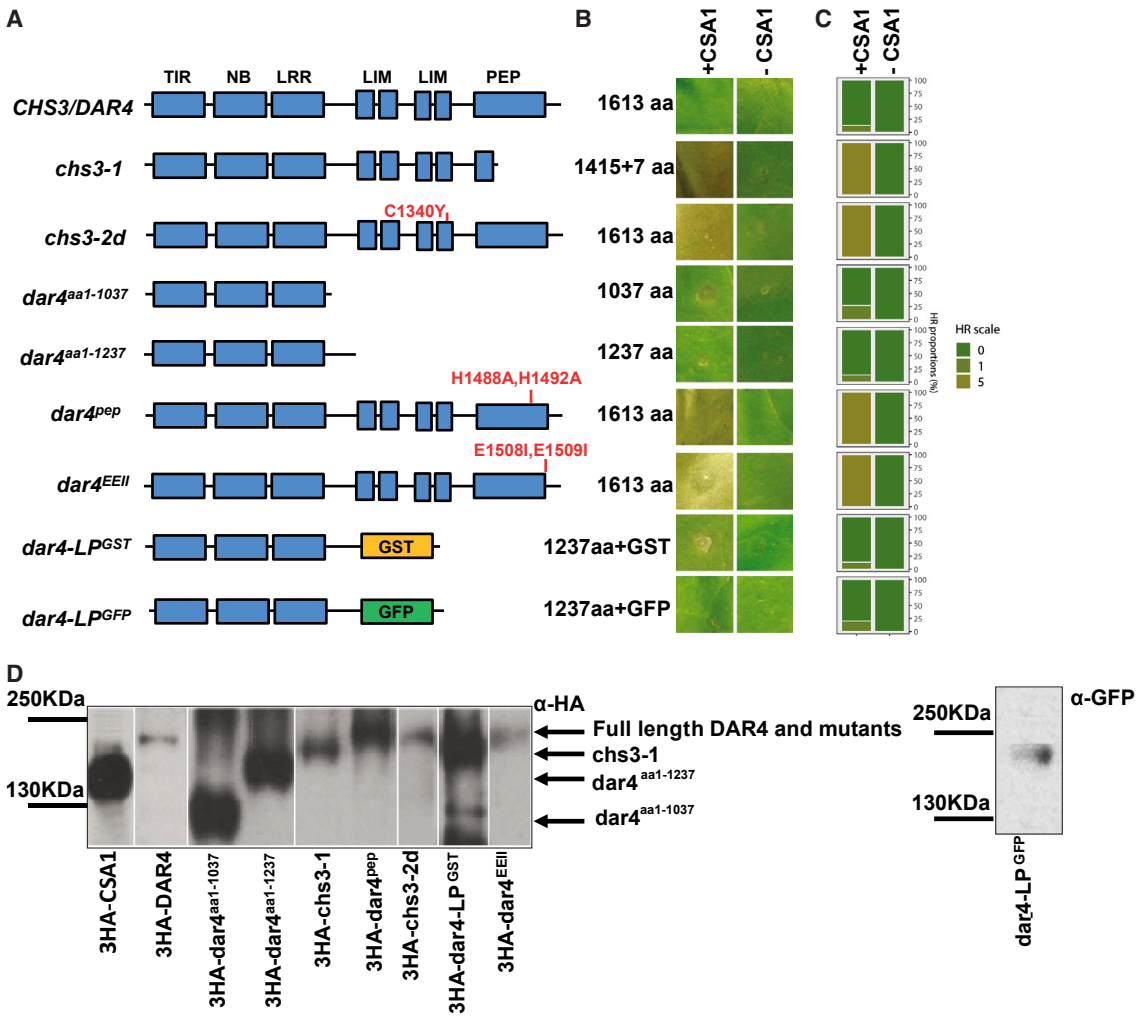

Figure 1. The LIM-peptidase region of DAR4 functions as an integrated decoy

(A) Diagram of known protein motifs of DAR4 and mutant and chimeric forms used to test hypersensitive responses. TIR, Toll, and interleukin-1 receptor homology regions; NB, NB-ARC nucleotide-binding; ARC, APAF-1,R proteins, and CED-4 domains; LRR, leucine-rich-repeat domain; LIM, LIN11, Isl1, and MEC3 domains; each Zn finger of the two LIM domains is represented; PEP, zinc-metallopeptidase region with AHEMMHA-EE active site; GST, glutathione S-transferase; GFP, green fluorescent protein. Red letters indicate the positions of mutated amino acid codons. C1340Y is in the fourth Zn-finger of the LIM repeats. H1488, H1492, E1508, and E1509 are in the HEMMA and EE motifs of the peptidase active site. The diagram is not to scale. Figure S2 shows the amino acid sequences and motifs of the DA1 family.

(B and C) Hypersensitive responses in *N. tabacum* leaves were assessed at 4 days post-infection. Images represent typical samples of three replicates. DAR4 and variants in (A) were co-expressed as 3HA-tagged proteins with (B) or without (C) CSA1. Quantified HR responses[29] are shown by the stacked bars are color coded to show the percentage of each cell death scale (0–5) in triplicated samples. Yellow represents the presence of HR, and green represents the absence of HR.

(D) Immunoblots showing expression levels of 3HA-tagged CSA1 and CHS3/DAR4 variants in leaf infection assays in the left panel and dar4-LP^{GFP} in the right immunoblot. 3HA-DA1 proteins were detected by HRP-coupled anti-HA antibodies, and GFP-tagged dar4-LP^{GFP} was detected with HRP-coupled anti-GFP antibodies. To accommodate large differences in expression of 3HA-DAR4 deletions and mutants, different loadings on separate gels were electrophoresed in order to detect protein bands.

between the CHS3/DAR4 LP domain and other family members targeted by putative effectors. The protein sequence relationships and domains of the eight DA1 family members are shown in Figures 2A and S2 and Tables S1 and S2. DAR3 is most closely related to DAR4. DAR3 and DAR7 are characterized by the absence of ubiquitin interaction motifs (UIMs) and may not be functional DA1 family peptidases.[23] We tested whether DA1 family LP domains caused HR responses by fusing LP domains of the seven other DA1 family members with the NLR region of CHS3/DAR4 (Figure 2B), co-expressed with CSA1, and HR in *N. tabacum* assessed. dar4-LP (DA1, DAR1, DAR2, DAR3, and DAR7) did not cause HR, with phenotypes that were the same as wild-type CHS3/DAR4 (Figures 2B and 2C). In contrast, dar4-LP(DAR5) and dar4-LP(DAR6) fusions caused HR (Figures 2B and 2C). Fusions of the CHS3/DAR4 NLR region with the unrelated proteins, dar4-LP^{GST} and dar4-LP^{GFP}, also did not lead to HR (Figures 1B–1D). To exclude the possibility that swapped DA1 family LP domains could not generate an

Please cite this article in press as: Gu et al., The integrated LIM-peptidase domain of the CSA1-CHS3/DAR4 paired immune receptor detects changes in DA1 peptidase inhibitors in *Arabidopsis*, Cell Host & Microbe (2023), https://doi.org/10.1016/j.chom.2023.04.009

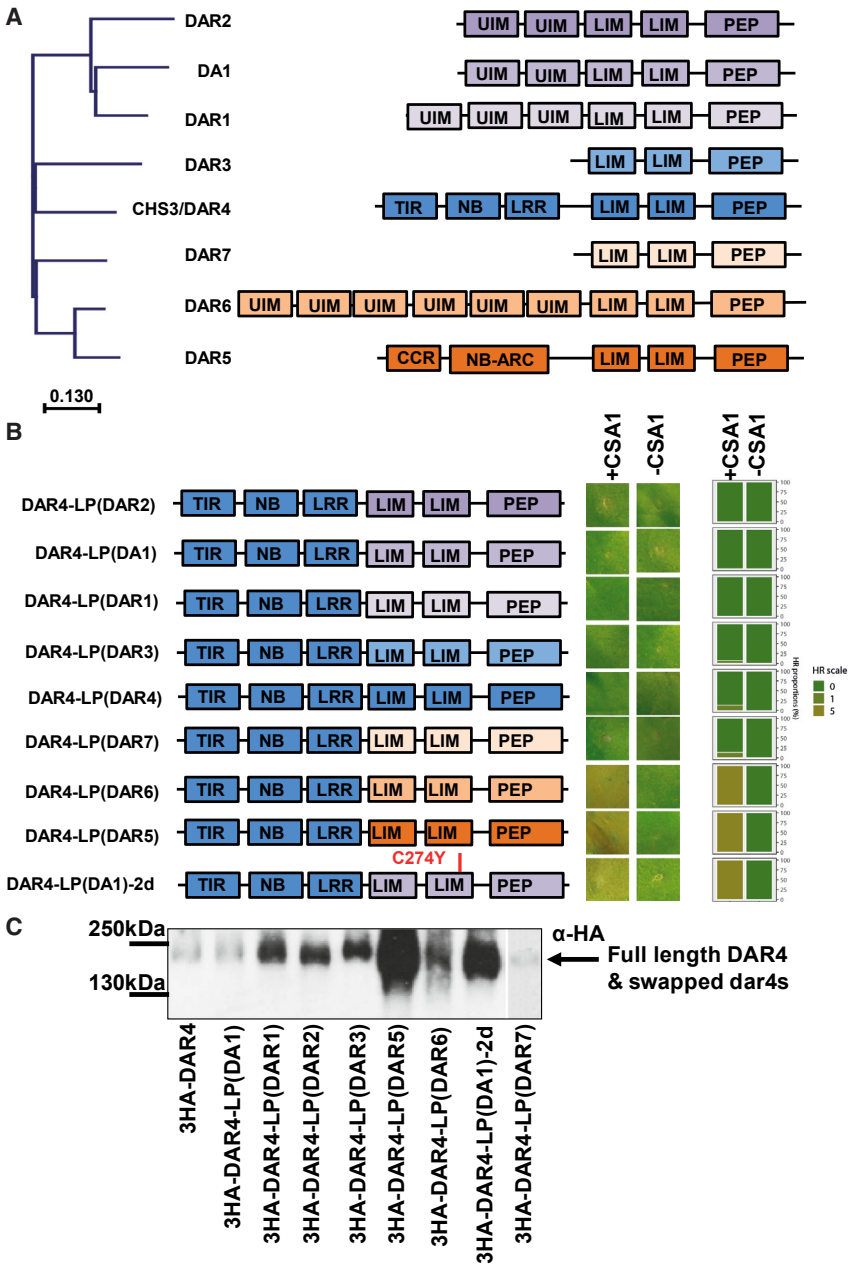

Figure 2. Domain swaps of LIM-peptidase regions of DA1 family members into DAR4 elicit HR responses

(A) Left: neighbor-joint phylogenetic tree of amino acid sequences of the LIM-peptidase region from the DA1 family in *Arabidopsis* accession Col-0. The distance scale is shown at the bottom of the panel. Right: diagram of the structural motifs of members of the DA1 family in *Arabidopsis thaliana* Col_0. UIM, ubiquitin interaction motif; LIM domains; PEP, peptidase domain; TIR-NB-ABC-LRR domains; RPW-8-like coiled-coil domain.

(B) Diagram of LIM-peptidase regions of DA1 family members swapped with that of DAR4. The colors indicate the different LIM-peptidase (LP) regions of family members in 3HA-tagged chimeric DAR4 proteins. DAR4-LP(DA1)-2d is DAR4 containing the LIM-peptidase region of DA1 with the DA1 C274Y amino acid change, shown in red.

(C) Hypersensitive responses (HRs) of chimeric DAR4 proteins expressed with and without CSA1 in *N. tabacum leaves*. The right panel shows quantified HR responses. The stacked bars are color coded to show the percentage of each cell death scale (0–5) in triplicated samples. Yellow represents the presence of HR, and green represents the absence of HR.

(D) Immunoblot showing expression levels of 3HA-tagged domain-swap DAR4 proteins in *N. tabacum* leaves. 3HA-DA1 proteins were detected by anti-HA-HRP antibodies. The right lane is from a separate gel with higher loading to detect the relatively low levels of 3HA-DAR4-LP(DAR7) expression.

HR, a mutant of dar4-LP(DA1) called dar4-LP(DA1)-2D with an amino acid alteration (DA1 C274Y) corresponding to the mutation in *chs3-2D* was tested. Strong HR was observed on co-expressing this protein with CSA1 (Figure 2B and 2C), demonstrating the capacity of fusions of DA1 family LP domains to cause HR. As DA1 is more distantly related to CHS3/DAR4 compared with DAR3 and DAR7 (Figures 2A and S2), the LP domains of DA1, DAR1, DAR2, DAR3, and DAR7 may all share a functionally conserved potential with CHS3/DAR4 to trigger HR when fused to the CHS3/DAR4 NLR region. Therefore, CHS3/DAR4 is probably an R protein for these family members. As DAR5 and DAR6 LP fusions cause HR when fused to CHS3/DAR4, they may be structurally and functionally different from other family members.

The LIM-peptidase domain of DAR4 lacks the activity of DA1 family peptidases

DA1, DAR1, and DAR2 are functionally redundant members of the DA1 family in Arabidopsis (Figure 2A) and share their peptidase substrates.[21,23] DA1 was selected to represent the activities of DAR1 and DAR2 in comparison to CHS3/DAR4. To test whether the LP domain of CHS3/DAR4 shares peptidase substrates with DA1, the LP domain of CHS3/DAR4 was swapped with that of DA1 to make da1-LP(DAR4) (Figure 3A) and its potential to cleave the Big Brother E3 ligase (BB-3FLAG) in Arabidopsis *da1-ko1dar1-1* leaf protoplasts was tested. No cleavage of BB-3FLAG was detected (Figure 3B), revealing functional differences between LP domains of DA1 and CHS3/DAR4.

As there was functional conservation of the LP domains of DA1 and CHS3/DAR4 with respect to triggering HR in *N. tabacum* (Figure 2B), smaller regions of the CHS3/DAR4 LP domain were swapped with that of DA1 and tested for peptidase activity (Figure 3A). Neither the LIM nor the peptidase domain of CHS3/DAR4 in DA1 catalyzed BB cleavage (Figure 3B). However, domain swaps of smaller regions, comprising each of the four single zinc fingers of the LIM and LIM-like domains, a conserved region between the LIM-like domain and the peptidase active

Please cite this article in press as: Gu et al., The integrated LIM-peptidase domain of the CSA1-CHS3/DAR4 paired immune receptor detects changes in DA1 peptidase inhibitors in *Arabidopsis*, Cell Host & Microbe (2023), https://doi.org/10.1016/j.chom.2023.04.009

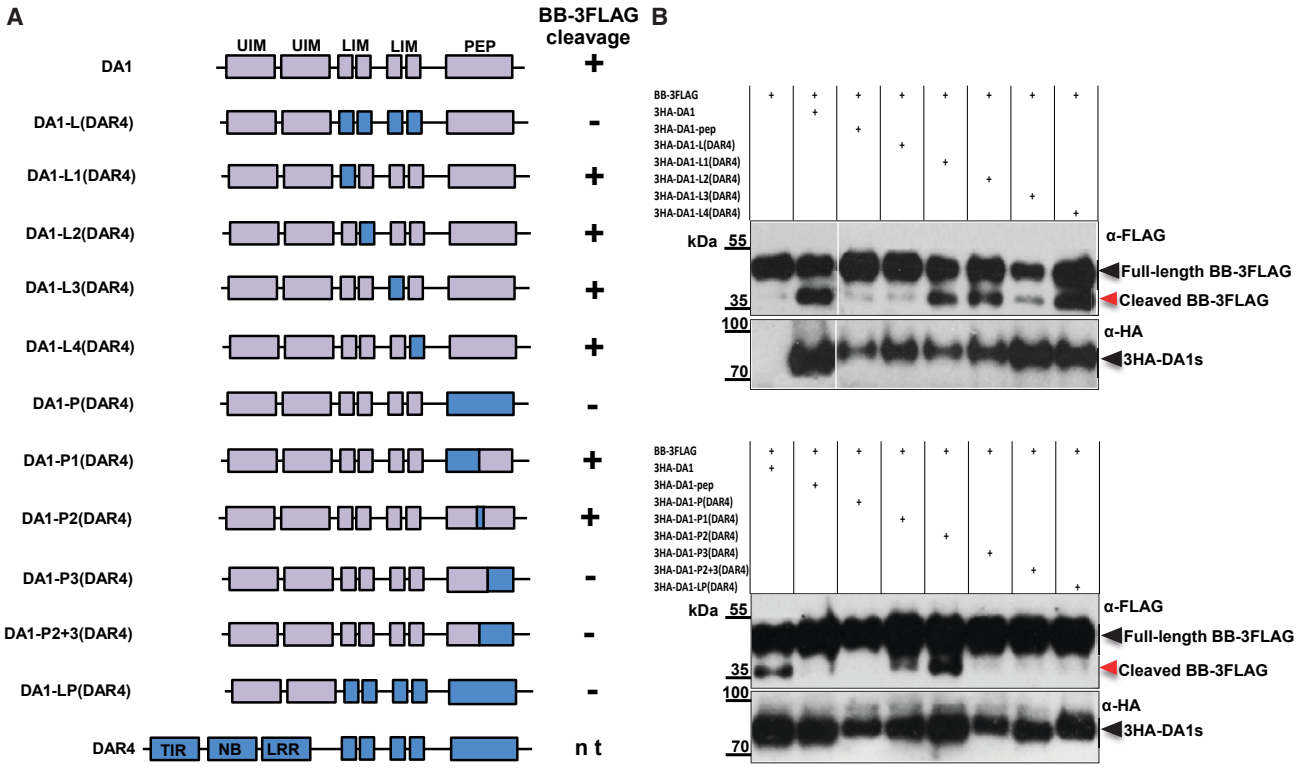

Figure 3. Peptidase activities of LIM-peptidase regions of DAR4 in chimeric DA1 proteins

(A) Diagram of chimeric 3HA-DA1 proteins used to test peptidase activities. Lilac, DA1 regions; blue, CHS3/DAR4 regions. The domain names are described in the legend to Figure 1. The diagram is not to scale. + shows BB-3FLAG cleavage; –, no cleavage; nt, not tested.

(B) Immunoblots of BB-3FLAG cleavage reactions in transfected Arabidopsis *da1dar1* mesophyll protoplasts using 3HA-DA1 chimeric proteins described in (A). 3HA-DA1 is a positive control and the 3HA-DA1 peptidase mutant (3HA-DA1 pep) is a negative control. BB-3FLAG proteins were detected by anti-FLAG-HRP antibodies. 3HA-DA1 proteins were detected by anti-HA-HRP antibodies. The positions of full-length (black arrow) and cleaved (red arrow) BB-FLAG proteins are indicated. The upper blot was split to remove a duplicated 3HA-DA1 + BB-3FLAG loading sample. All samples are from the same immunoblot exposed for the same time.

site, and a small active site region of DA1 in the CHS3/DAR4 C-terminal region all efficiently cleaved BB-3FLAG in the DA1 protein context (Figure 3B). Thus, functional conservation was limited to smaller regions of the LP of DA1 and CHS3/DAR4. A failure to ubiquitylate the DA1 domain-swap proteins was ruled out as an explanation for reduced BB cleavage by the domain-swap proteins as they were all equally ubiquitylated (Figure S3). This functional variation between the LP domains of DA1 and CHS3/DAR4 and the functional conservation of DA1, DAR1, and DAR2[32] indicated that these three family members may not be direct targets of putative effectors sensed by the CHS3/DAR4 R protein. The more closely related family members (DAR3 and DAR7), which also did not cause HR when their LP regions were fused to CHS3/DAR4 (Figure 2B), may have a more direct role in CHS3/DAR4-mediated resistance.

DA1 family peptidases confer susceptibility to diverse plant pathogens

The functions of DAR3 and DAR7 in the context of plant growth are not known, and the possible roles of DA1 and DAR1 family members in pathogen responses have also not been studied. We assessed the involvement of *DA1* and *DAR1* in pathogen growth by measuring the growth of the bacterial pathogen *Pseudomonas syringae* pathovar *tomato* (*Pst*) strain DC3000 and the oomycete pathogen *Hyaloperonospora arabidopsidis* (*Hpa*) isolate Noco2 in Arabidopsis *da1-kodar1-1* loss-of-function double mutants and *DA1* over-expression lines in Col-0. The *da1-ko1* loss-of-function mutant in Col-0 showed no significant differences in *Pst* DC3000 growth compared with wild-type plants, but the double *da1-ko1dar1-1* mutant supported much lower levels of pathogen growth (Figure 4A). The *dar1-1* single mutant showed *Pst* DC3000 growth levels intermediate between the wild-type and the *da1-ko1dar1-1* double mutant (Figure 4A; Table S3.1). More extreme reductions in pathogen growth were observed after infection by *Hpa* isolate Noco2. The double-mutant *da1-ko1dar1-1* exhibited strongly reduced Noco2 growth, whereas the two single mutants exhibited moderately reduced Noco2 growth compared with wild-type Col-0 (Figure 4B; Table S4). No significant differences in Noco2 growth were detected in two independent *DA1* over-expression lines *ox-DA1-1.3* and *ox-DA1-4.13* (Figure 4B; Table S4). *DA1* and *DAR1* are therefore likely to be susceptibility genes redundantly required for optimal growth of bacterial and oomycete pathogens in *Arabidopsis*.

As *CHS3/DAR4* and *CSA1* are responsible for the genetic activity of the *WRR5* resistance locus for *A. candida* AcEm2,[4]

Please cite this article in press as: Gu et al., The integrated LIM-peptidase domain of the CSA1-CHS3/DAR4 paired immune receptor detects changes in DA1 peptidase inhibitors in *Arabidopsis*, Cell Host & Microbe (2023), https://doi.org/10.1016/j.chom.2023.04.009

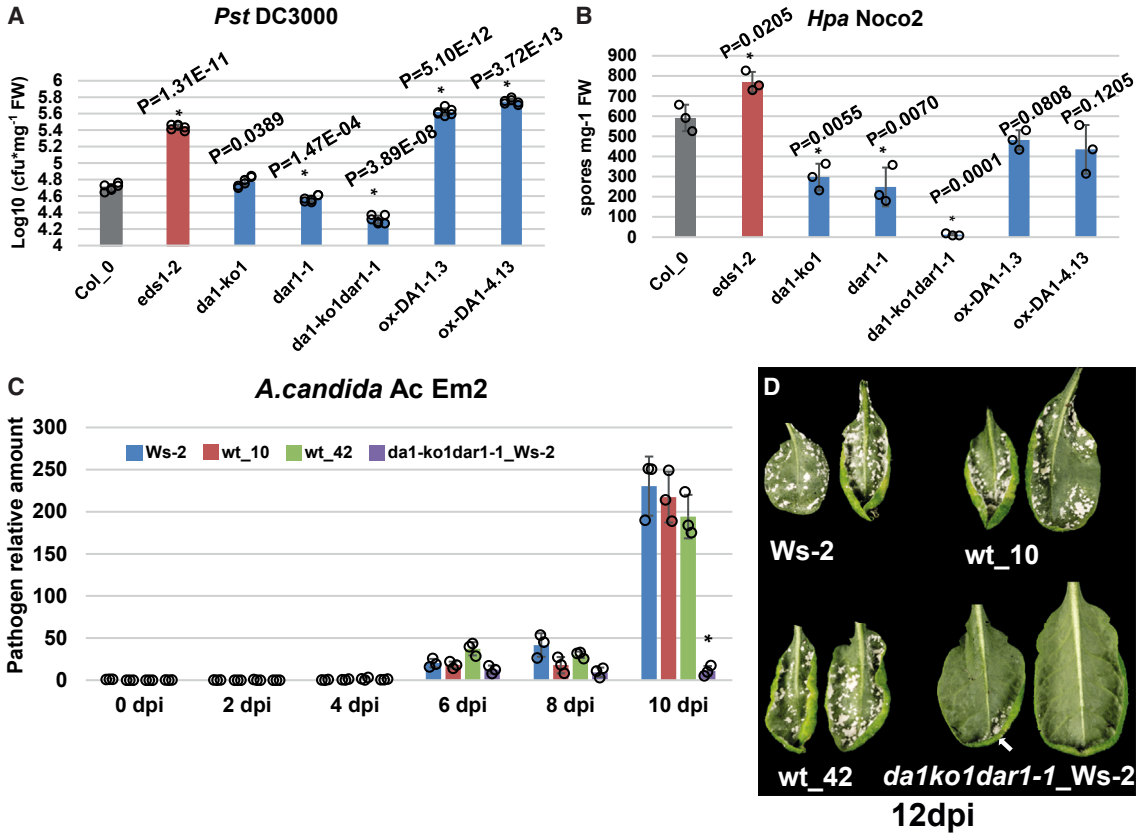

Figure 4. *DA1* and *DAR1* facilitate growth of bacterial and oomycete pathogens in *Arabidopsis*

(A) *Pseudomonas syringae Pst* DC3000 growth on *Arabidopsis* Col-0 *da1* and *dar1* knockout lines and *35S::DA1* overexpressing lines. CFUs, colony-forming units per mg fresh weight of inoculated leaves. The *eds1-2* mutant was used as a standard susceptible control.

(B) *Hyaloperonospora arabidopsidis* (*Hpa*) race Noco2 growth on *Arabidopsis* Col-0 *da1* and *dar1* knockout lines and *35S::DA1* over-expressing lines. FW, fresh weight of spores in infected plants. The *eds1-2* mutant was used as a susceptible control.

(C) Time course of *Albugo candida* AcEm2 growth on *Arabidopsis* Ws-2 and backcross lines with Col-0 *da1dar1*. wt-10 and wt-44 contain wt DA1 and DAR1 loci from Ws-2 in BC7F2, while *da1-ko1dar1-1*_Ws-2 contains homozygous Col-0 *da1dar1* mutants in BC7F2. Infection progress was measured using the ratio of pathogen DNA to host DNA levels. dpi, days post-infection. Statistical significance was at *p < 0.01 based on a two-tailed Student's t test. Comparisons of pathogen levels were those in Ws-2 at 0 dpi. Error bars represent SD of the mean.

(D) Image of *Albugo candida* AcEm2 growth on leaves of Ws-2 and backcrossed lines at 12 dpi leaves. The white areas are Em2, and the arrow indicates a small amount of pathogen growth on the *da1-ko1dar1-1*_Ws-2 backcrossed line.

putative effector molecules detected by CHS3/DAR4 may modulate the activities of DA1 family members to support pathogen growth. To test this, *da1-ko1dar1-1* double mutants in Col-0 were backcrossed into the *Arabidopsis* Ws-2 accession, which is susceptible to *A. candida* AcEm2. In BC7F2, a homozygous double-mutant line (*da1-ko1dar1-1*_Ws-2) and two lines homozygous for the *Ws-2* wild-type *DA1* and *DAR1* alleles (wt-10 and wt-42) were tested for AcEm2 growth. This was strongly reduced in the *da1-ko1dar1-1* line after 8 days post-inoculation (dpi), whereas both wild-type *DA1 DAR1* Ws-2 lines and the original Ws-2 parental line supported similar high levels of pathogen growth (Figures 4C and 4D; Table S5). AcEm2 growth was also assessed in two independent DA1 over-expression lines in Ws-2. No differences in AcEm2 growth were detected (Figure S4A; Table S5). To avoid the possibility that background mutations may influence pathogen growth in these experiments, PstDC3000 growth was tested in Ws-2 with the *da1dar1* double mutant. This showed similar *Pst* DC3000 growth reductions in the *da1-ko1dar1-1* double mutant in Col-0 (Figures 4A and S4B; Table S3.2), demonstrating the dependence of pathogen growth on functional DA1 and DAR1. These observations support the hypothesis that CHS3/DAR4 may detect effectors that modulate, directly or indirectly, DA1 and DAR1 activity to promote pathogen growth.

Leaf cell endoreduplication induced by *A. candida* AcEm2 infection requires DA1 family peptidase activity

DA1, *DAR1*, and *DAR2* redundantly promote the transition from mitosis to endoreduplication during organ growth by cleavage of positive regulators of mitosis.[21,23,32,33] Endoreduplication is also induced during infection to facilitate pathogen growth.[34–36] To test whether DA1 family peptidase activities contribute to pathogen-induced endoreduplication, ploidy levels of Arabidopsis leaf cells during infection by oomycete pathogen *A. candida* AcEm2 were measured in susceptible Ws-2 and the wt-42 *DA1 DAR1* Ws-2 BC7F2 wild-type lines. Both lines showed similar

Please cite this article in press as: Gu et al., The integrated LIM-peptidase domain of the CSA1-CHS3/DAR4 paired immune receptor detects changes in DA1 peptidase inhibitors in *Arabidopsis*, Cell Host & Microbe (2023), https://doi.org/10.1016/j.chom.2023.04.009

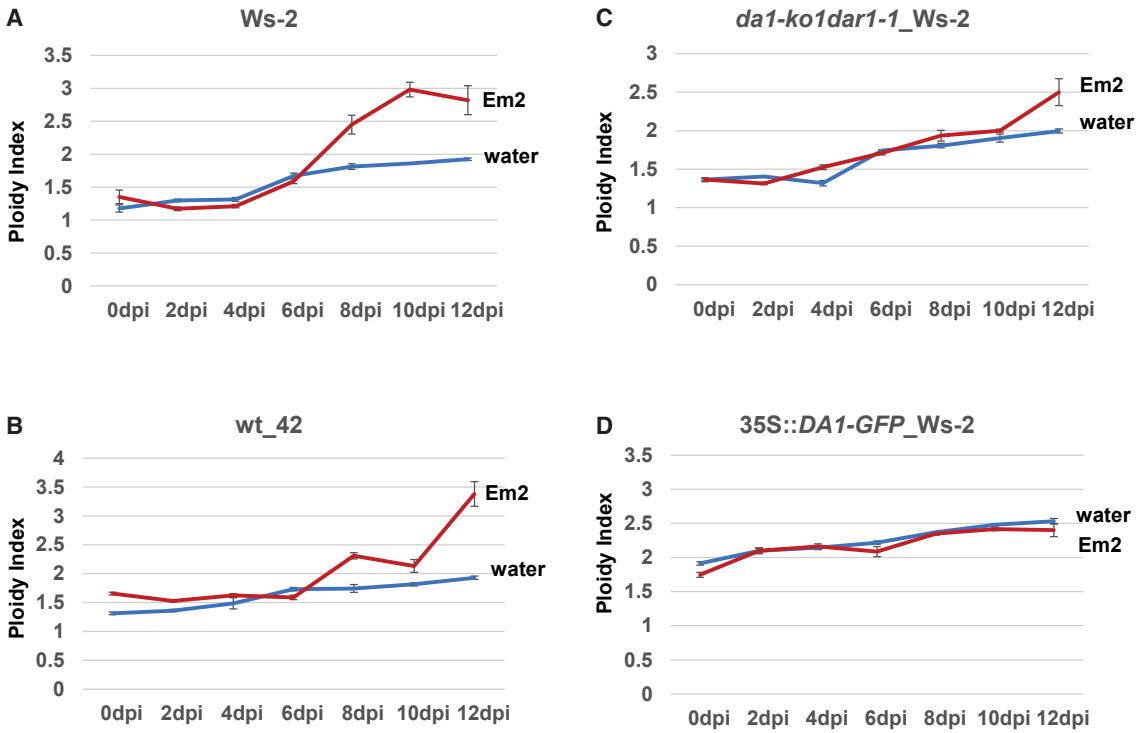

Figure 5. Increases in leaf ploidy levels during *A. candida* Ac Em2 infection of *Arabidopsis thaliana* are dependent on DA1 and DAR1

The graphs show ploidy levels of infected leaf cells during *A. candida* Ac Em2 infection of *Arabidopsis thaliana* Ws-2 wt, wt-42, *da1-ko1dar1-1*_Ws-2 backcross line leaves, and a *35S::DA1* over-expression line in Ws-2 up to 12 days post infection (dpi). The red lines show inoculation with AcEm2 spores and the blue lines show mock inoculation with water.

(A) Wild-type Ws-2 ploidy index.

(B) Ws-2 backcross line wt-42 containing wild-type Ws-2 *DA1* and *DAR1* alleles.

(C) Ws-2 backcross line containing loss-of-function Col-0 *da1-ko1* and *dar1-1* genes.

(D) *35S::DA1* over-expression line. Note the increased ploidy index at 0 days post infection.

Error bars represent SD of the mean.

increases in leaf cell ploidy between 8 and12 dpi (Figures 5A and 5B; Table S6). In comparison, the *da1-ko1dar1-1* double mutant in Ws-2 exhibited delayed ploidy increases at 12 dpi (Figure 5C; Table S6). A DA1 over-expression line (35S::DA1-GFP_Ws-2) exhibited higher ploidy levels in both mock- and AcEm2-infected leaves at early stages of infection compared with Ws-2 and wt-42 (Figure 5D; Table S6), whereas these two lines showed higher ploidy levels than 35S::DA1-GFP_Ws-2 at 10 and 12 dpi (Figures 5A and 5B; Table S6), although AcEm2 growth was not increased in DA1 overexpression lines (Figure S4A; Table S5). This suggested that there is sufficient DA1 in wild-type leaves to support the full extent of pathogen growth in these conditions and that elevated ploidy levels at early stages of AcEm2 infection do not promote growth. These data show that *A. candida* AcEm2 promoted DA1- and DAR1-mediated ploidy increases between 8 and 10 dpi, which are required for pathogen growth (Figure 4C).

DAR3 and DAR7 inhibit the peptidase activities of DA1 family peptidases

The difference *in planta* activities of LP domains from DAR4 and DA1, DAR1, and DAR2 (Figures 3A and 3B) suggested that DAR3 and DAR7, which are more closely related to DAR4, may be potential targets of putative pathogen effectors that are detected by the ID of the CHS3/DAR4 immune receptor. DA1 interacts with itself to modulate its peptidase activity.[27] Similarly, DAR3 also interacted with itself and DA1, DAR1, and DAR2 in co-immunoprecipitation assays using protoplast-expressed proteins (Figure 6A). DAR3 also interacted with the CHS3/DAR4 LP region (CHS3/DAR41127-1613) (Figure S5). To dissect these interactions, DAR3-GFP was co-expressed with 3HA-DA1 and its substrate BB-3FLAG in Col-0 *da1dar1* mesophyll protoplasts to test its influence on BB-3FLAG cleavage. BB-3FLAG cleavage by 3HA-DA1 was strongly reduced by DAR3-GFP (Figure 6B). The DA1 peptidase mutant DA1-pep had no effect on reducing wild-type DA1 peptidase activity on BB-3FLAG cleavage when co-expressed at different levels with DA1 (Figure 6C), indicating that DAR3 had a specific inhibitory effect on DA1 peptidase activity. Co-expression with DAR7 also reduced DA1 peptidase activity but to a lower extent than DAR3 (Figure 6D).

As *DAR3* is the closest homolog of *CHS3/DAR4* encoded in *Arabidopsis* genomes (Figure 2A), and because it inhibited DA1 peptidase activity, we assessed the specificity of LP domains on this inter-family modulation of DA1 peptidase activity. The LP domains of DA1, DAR3, and CHS3/DAR4 were swapped and tested for their effects on DA1 peptidase activity as GFP fusion proteins. Inhibition of DA1 peptidase activity by DAR3-LP(CHS3/DAR4), comprising the LP domain of CHS3/DAR4 in

Please cite this article in press as: Gu et al., The integrated LIM-peptidase domain of the CSA1-CHS3/DAR4 paired immune receptor detects changes in DA1 peptidase inhibitors in *Arabidopsis*, Cell Host & Microbe (2023), https://doi.org/10.1016/j.chom.2023.04.009

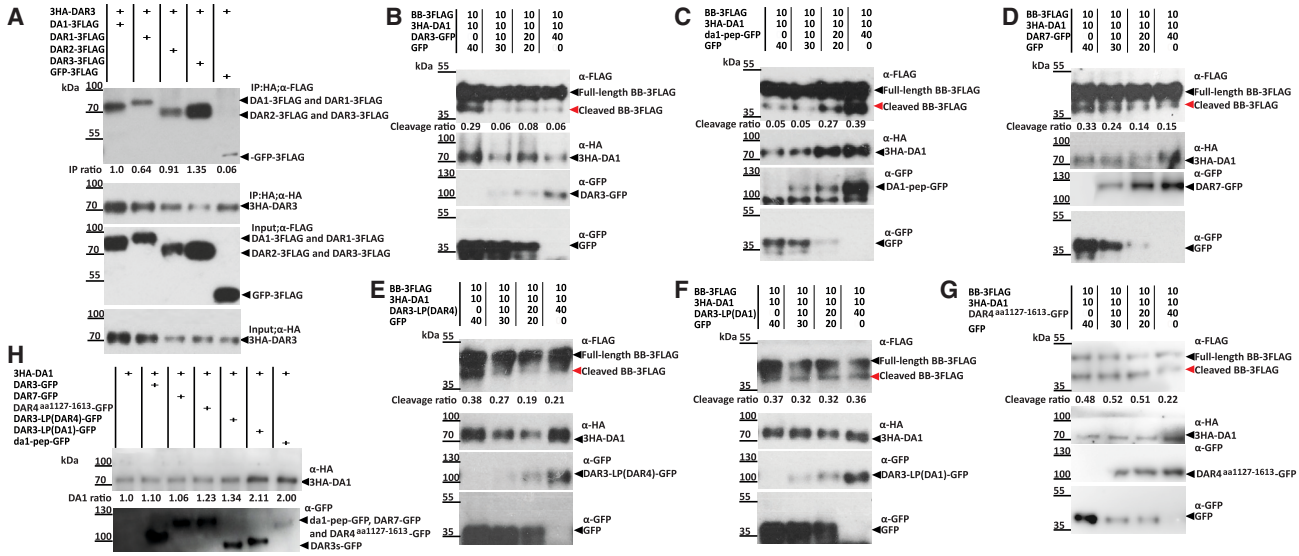

Figure 6. DAR3 and DAR7 family members inhibit DA1 peptidase activity

Immunoblots of Col-0 *da1-ko1dar1-1* transfected Arabidopsis mesophyll protoplasts. The numbers above each lane show the fold levels of 10 μg units of transfected DNA *35S::GFP* was used to balance total DNA levels to 60 μg per transfection. The red arrows indicate cleaved BB-3FLAG while the black arrows indicate intact BB-3FLAG.

(A) Co-immunoprecipitation of 3HA-DAR3 and DA1-, DAR1-, and DAR2-3FLAG.

(B) Progressive inhibition of 3HA-DA1 peptidase activity on BB-3FLAG by increasing levels of DAR3-GFP.

(C) Increased levels of inactive DA1-peptidase mutant-GFP do not inhibit 3HA-DA1 peptidase activity on BB-3FLAG.

(D) DAR7-GFP also progressively inhibits 3HA-DA1 peptidase activity on BB-3-FLAG.

(E) Progressive reduction of 3HA-DA1 peptidase activity on BB-3FLAG by DAR3-GFP containing the LIM-peptidase region of DAR4.

(F) DAR3-GFP containing the LIM-peptidase region of DA1 does not affect 3HA-DA1 peptidase activity on BB-3FLAG.

(G) The LIM-Peptidase domain of DAR4 (DAR4$^{1127\text{-}1613}$ – GFP) does not reduce 3HA-DA1- mediated cleavage of BB-3FLAG.

(H) 3HA-DA1 protein levels are not affected by co-expression with DAR3-GFP and LIM-Peptidase-GFP proteins.

DAR3, was compared with DAR3-LP(DA1) as a control. There was a stronger reduction in DA1 peptidase activity by DAR3-LP(CHS3/DAR4) compared with DAR3-LP(DA1) (Figures 6E and 6F). Figure 6G shows that the LP region of CHS3/DAR4-GFP alone reduced BB-3FLAG cleavage to a lower extent than DAR3-GFP (Figure 6B), suggesting that DAR3 had a more specific inhibitory effect on DA1-mediated cleavage of BB-3FLAG. Figure 6H showed that 3HA-DA1 protein levels were not affected by co-expression with DAR3-GFP and LP-GFP proteins. Inhibition of DA1 peptidase activity by LP domains of DAR3 and CHS3/DAR4 in the context of the DAR3 protein is consistent with the high degree of sequence conservation between DAR3 and CHS3/DAR4 LP domains. These observations linked the inhibition of DA1 peptidase activity by DAR3 with the function of CHS3/DAR4 as an integrated decoy.

DAR3 is involved in resistance to multiple pathogens

As DA1 family peptidase activity promotes pathogen growth and is required for host ploidy increases during infection (Figures 4A–4D and 5A–5D) and because DAR3 inhibits DA1 peptidase activities (Figure 6B), one plausible mechanism by which pathogens could increase DA1 activity to promote infection may involve reducing DAR3-mediated inhibition of DA1. This was tested by expressing *DAR3-GFP* from the *35S* promoter in the susceptible Ws-2 accession and measuring DAR3-GFP protein stability during AcEm2 infection. DAR3-GFP protein levels were rapidly depleted in AcEm2-infected but not in water-treated plants, with reduced levels from 2 dpi, very low levels between 4 and 6 dpi, and a slight increase between 8 and 10 dpi (Figure 7A). 3HA-DA1 stability was not affected by AcEm2 infection (Figure 7A). AcEm2 growth was measured on independent *DAR3-GFP* over-expression lines and in the *dar3* CRISPR knockout lines *dar3-2* and *dar3-3* in Ws-2 (described in Figure S6). Over-expression of *DAR3* reduced AcEm2 growth at 8 and 10 dpi, whereas growth on the *dar3* loss-of-function lines was elevated at 6, 8, and 10 dpi (Figures 7B and 7C; Table S7). The *dar3-2* allele was more effective at promoting AcEm2 growth. These data were supported by the promotion of both *Pst* DC3000 and *Hpa* Waco9 and *Pst DC3000* growth by a *dar3-1* loss-of-function T-DNA allele in Col-3 (Figures 7D, 7E, and S6; Tables S8 and S9) and reduction in the growth of *Pst* DC3000 in Ws-2 *DAR3* overexpression lines in the Ws-2 accession (Figure 7F; Table S10). These results suggest that *DAR3* reduced the growth of several pathogens and its rapid reduction during the early stages of AcEm2 infection facilitated pathogen growth.

To ensure that these patterns of DAR3 reduction were specific to CSA1-CHS3/DAR4-mediated ETI responses and were not PTI responses, levels of 3HA-DAR3, 3HA-CHS3/DAR4$^{1127\text{-}1613}$, and 3HA-DA1 protein were compared in Ws-2 infected with *A. candida* AcEm2 (resisted by CHS3/DAR4) and *A. candida* AcEx1(CHS3/DAR4 susceptible). Figure S7 shows the expected reduction in 3HA-DAR3 levels at 2 and 4 dpi in response to AcEm2 infection, although no changes were seen during infection with AcEx1. 3HA-DA1 and 3HA-CHS3/DAR4$^{1127\text{-}1613}$ protein

Please cite this article in press as: Gu et al., The integrated LIM-peptidase domain of the CSA1-CHS3/DAR4 paired immune receptor detects changes in DA1 peptidase inhibitors in *Arabidopsis*, Cell Host & Microbe (2023), https://doi.org/10.1016/j.chom.2023.04.009

CellPress
OPEN ACCESS

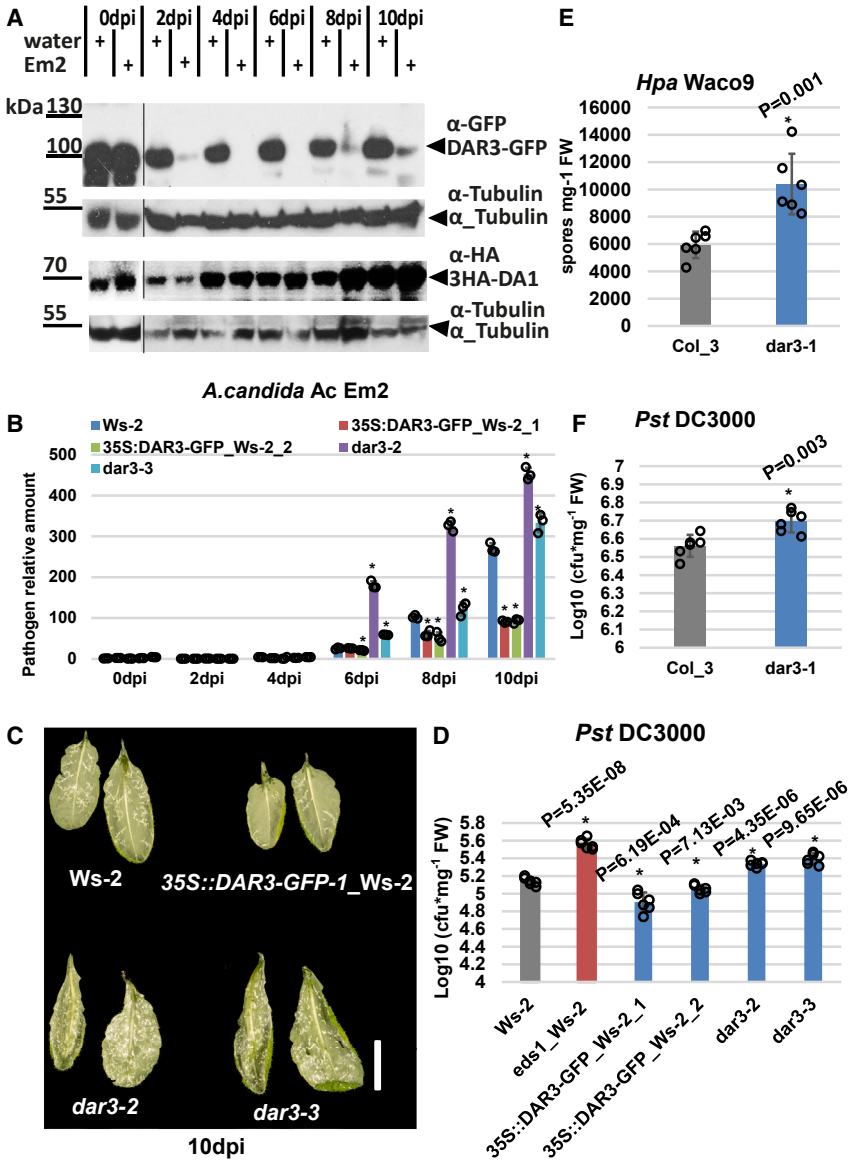

Figure 7. *DAR3* reduces pathogen growth

(A) The immunoblot shows a time course of DAR3-GFP and 3HA-DA1 protein levels during *A. candida* Ac Em2 infection of Arabidopsis Ws-2 leaves expressing *35S::DAR3-GFP* or *35S::3HA-DA1*. Transgenic seedlings were treated with Em2 spores or water as a control. Tubulin was used as a loading control for plant protein levels. dpi, day post-inoculation. The panels on the left showing DAR3-GFP levels at 0 dpi were exposed for a shorter time than the other panel.

(B) Time course of *A. candida* Ac Em2 growth on *Arabidopsis thaliana* Ws-2 and *DAR3* over-expression and CRISPR mutant lines. Infection progress was measured using the ratio of pathogen DNA to host DNA levels. dpi, days post-inoculation. Statistical significance was at *$p < 0.01$ from a two-tailed Student's t test.

(C) Image of *A. candida* Ac Em2 growth on leaves of Ws-2 and DAR3 over-expression and mutant lines at 10 dpi leaves. The white regions are Em2.

(D and E) The *dar3-1* mutant in Col-3 is more susceptible to *Pst* DC3000 (D) and *Hpa* variety Waco9 (E). Statistical significance was at *$p < 0.05$ based on a two-tailed Student's t test. Error bars represent SD of the mean.

(F) *Pst* DC3000 growth on *Arabidopsis* Ws-2 and *DAR3* over-expression and CRISPR knockout mutant lines. CFUs, colony-forming units per mg fresh weight of inoculated leaves. The *eds1*_Ws-2 mutant was used as a standard susceptible control. Individual data points are shown, and p values are from Student's t tests.

levels were not affected by either pathogen. This established that reduced DAR3 levels guarded by CSA1-CHS3/DAR4 (Figures 7A and S7) were a specific ETI response.

Sequence diversity of the DA1 peptidase family

Sequence variation at *CSA1&CHS3/DAR4* loci as well as *DA1* and *DAR3* was assessed using long-read-based assemblies of 27 diverse *Arabidopsis* accessions from the 1001 Genomes Plus project. Thirteen accessions had near-identical *CSA1* alleles (clade 1), whereas 12 accessions had more variable clade 2 *CSA1* alleles (Table S11). Accession KBS-Mac-74 (1741) had a distinctive clade 1-like *CSA1* allele with several large indels, whereas accession Qar-8a (9764) had a clade 2 *CSA1* allele with a large C-terminal deletion. Accession Elh-2 (22004) lacked the *CSA1-CHS3/DAR4* locus. Only *CHS3/DAR4* alleles with complete LP ID were linked to complete clade 1 CSA1 alleles, as reported.[37] Two fusion points of the ID with the conserved *CHS3/DAR4* NLR domain were seen (Figure S8A), whereas accessions KBS-Mac-74 and ET-86.4 (accession 22007) had remnant LP sequence similarities containing large deletions. This indicated a possible loss of the ID in these accessions that was consistent with pairing to clade 2 *CSA1* alleles.

As the *DAR3*-like ID in *CHS3/DAR4* is required for resistance to *Albugo*, based on guarding *DA1* family members, and as the *CSA1-CHS3/DAR4* pair exhibits balancing selection,[25,37] it is possible that *DA1*, an indirect target of putative effector(s), and *DAR3*, a possible direct target of putative effector(s) in accessions that are sensed by *CHS3/DAR4*, may also exhibit co-evolution due to pathogen pressure, compared with accessions that do not contain the ID. Although nucleotide diversity and Tajima's D, a measure of non-neutrality,[38] were lower for both *DA1* and *DAR3* genes in clade 2 accessions compared with clade 1 accessions with complete *CSA1* and *CHS3/DAR4* loci, neither clade was different from randomly permuted sets of accessions ($p > 0.05$, Figure S8B). Therefore, we cannot conclude from these analyses that members of the *DA1* family sensed by *CSA1/CSH3* are also subject to co-evolution. However, the lower nucleotide diversity in DA1 compared with DAR3 supports DAR3 as a putative effector target (Figure S8C).

Please cite this article in press as: Gu et al., The integrated LIM-peptidase domain of the CSA1-CHS3/DAR4 paired immune receptor detects changes in DA1 peptidase inhibitors in *Arabidopsis*, Cell Host & Microbe (2023), https://doi.org/10.1016/j.chom.2023.04.009

Phylogenetic analyses of LP protein sequence diversity in the *Brassicaceae* showed the DA1 family formed two general clades: clade 1I comprised three subgroups of DA1, DAR1, and DAR2-like proteins with relatively low diversity: clade II has three subgroups of more diverse DAR3- and CHS3/DAR4-like, DAR5- and DAR6-like, and DAR7-like proteins that contain 8 NLR proteins (Figure S9; Table S12). Five DAR5-like proteins encoded by *B. juncea*, *B napus*, *B. oleracea*, and *R. sativus* clustered in one branch, suggesting a common origin. In contrast, DAR5 from *Arabidopsis* was closest to DAR6 from *Arabidopsis* and clustered with DAR6-like proteins from *Camelina sativa*, indicating an independent origin from the other five DAR5-like proteins. Therefore, at least three LP domains integrated at least three times in clade II DA1 family proteins, one for DAR4-like and two for DAR5-like, during the evolution and domestication of *Brassicaceae*. Multiple domain integrations and high protein diversity are consistent with the targeting of clade II proteins by pathogen effectors.[25,30] In clade II, the DAR5-like NLR proteins were clustered with DAR6, and two NLR-DAR4-like proteins were clustered with non-NLR-DAR4 and DAR3 proteins. Their common origin and functional conservation are consistent with NLR-CHS3/DAR4-like proteins being R proteins that detect effectors targeting DAR3-like proteins.

DISCUSSION

NLR fusions to LP domains are widespread in several major plant families,[10,11] but their roles in effector sensing and pathogen growth are unknown. Here, we show using domain swaps that the LP ID of the NLR CHS3/DAR4 paired R gene conferring resistance to the oomycete pathogen *Albugo candida* AcEM2 is an integrated decoy for the DA1 family member DAR3. DAR3 interacts with and inhibits the peptidase activities of DA1 family members, and pathogen infection leads to a potential effector targeting it, leading to its degradation. This increases DA1 peptidase activity, promoting host tissue endoreduplication and pathogen growth.

The LIM-peptidase-integrated domain of CHS3/DAR4 functions as a potential decoy for DA1 family members

The integrity of the LP ID of DAR4 is required to maintain a putative CHS3/DAR4 sensor and CSA1 executor resistance gene function in a poised state.[8,28,39] Swapping the LP domain of DAR4 with those of other family members showed that those from DA1, DAR1, DAR2, DAR3, and DAR7 did not cause HR, indicating shared features able to maintain this poised state of CSA1-CHS3/DAR4 (Figures 1A–1D and 2B). The LP domain of CHS3/DAR4 is therefore likely to be an ID, the integrity of which is reduced by putative effectors that may also influence other DA1 family members except for DAR5 and DAR6, which trigger CSA1-dependent HR responses when fused to CHS3/DAR4. Reciprocal swaps of LP domains showed that the full DAR4 LP domain does not cleave the DA1 substrate BB, although smaller fragments of the CHS3/DAR4 LP domain in DA1 have peptidase activity (Figure 3A and 3B), indicating limited functional conservation of the CHS3/DAR4 LP ID to DA1, DAR1, and DAR2 despite identical catalytic site sequences (Figure S2). Therefore, DAR3, which is most closely related to DAR4, and possibly DAR7 (Figure 2A), are more likely targets for putative effectors that affect LP integrity.

IDs are thought to arise by recombination and duplication of putative effector target genes with NLR domains,[30] and under such a scenario, DAR4 most likely arose from DAR3 in the *Brassicaceae* family[21] and was presumably selected to combat *Brassica*-specific pathogens such as *Albugo*. Only *Arabidopsis* and *Camelina sativa* had DAR4-like LP regions fused to an NLR, suggesting specific evolution of resistance to *Albugo* in these two taxa.

Of all NLR pairs surveyed in *Arabidopsis*, diversity is highest in the *CSA1/CHS3-DAR4* gene pair,[25] pointing to extensive co-evolution of changes in NLR-LIM peptidase pairs. Although *DAR3* was not particularly diverse in *Arabidopsis* accessions (Figure S8), different from what has been observed for other effector targets, analyses of LP ID sequence diversity in *Brassicaceae* showed relatively high levels of diversity in *CHS3/DAR4*, *DAR3*, and *DAR7* clades, the effector targets predicted to be sensed by CHS3/DAR4 (Figure S9). This high degree of diversity, in contrast to the lower level of diversity of *DA1*, *DAR1*, and *DAR2*, is consistent with DAR3 and DAR7 potentially being targets of pathogen effectors in the *Brassicaceae* that are subject to diversification and selection in the "arms race" between hosts and pathogens.[18,25]

DA1 family peptidases facilitate pathogen growth

According to models of intracellular immunity in plants,[18] if the DAR4/CHS3 LP ID functions as a decoy for other members of the DA1 family, then these members may facilitate or inhibit pathogen growth and therefore be targeted by pathogen effectors. Parasitic and mutualistic biotrophic growth can induce host cell endoreduplication, with ploidy changes accommodating colonization by supporting nutrient production in infected host cells (reviewed by Wildermuth et al.[36]). The peptidase activities of DA1, DAR1, and DAR2 redundantly limit cell proliferation and promote the transition from mitotic cell divisions to endoreduplication.[21,32] We could link this to pathogen growth by demonstrating that the *da1-ko1dar1-1* double mutant, which reduced endoreduplication during normal plant growth, also supported less bacterial and oomycete growth, whereas overexpression of DA1 increased bacterial pathogen growth (Figure 4A–4D). TCP14 and TCP15, substrates of DA1 peptidase,[23] promote mitotic progression. Mutations in TCP14 and TCP15 (Teosinte Branched 1-Cycloidea-PCF) transcription factors facilitate a powdery mildew infection,[36] consistent with pathogen infection increasing DA1 peptidase activity and reducing TCP14 and TCP15 protein levels. Interaction screens also identified several effectors from different pathogens that converge on TCP14 and TCP15[17,23] and TCPs form IDs,[25] establishing DA1 peptidase activities among this nexus of effector targets. This is consistent with the frequent identification of cell cycle regulatory proteins as interactors with diverse bacterial and fungal effectors,[40] emphasizing a central role for modulation of host cell cycle functions by pathogens and commensals in plants.

Reduction of DAR3 levels on pathogen growth promotes DA1 activity

As CHS3/DAR4 functions as an ID for other members of the DA1 family that promote pathogen growth, it is possible that the activities of DA1 family members are modulated by pathogen effectors to facilitate pathogen growth and that this is sensed by the

CHS3/DAR4 LP ID. In uninfected tissues, DAR3 interacts with DA1 and inhibits its peptidase activity (Figure 6B), whereas in infected tissues, DAR3 is rapidly destabilized (Figure 7A). There is widespread evidence that effectors influence host protein stability,[41] and this may account for the destabilization of DAR3. For example, some effectors have E3 ligase domains that promote ubiquitylation of host proteins, and some effectors bind to and suppress the activities of host E3 ligases. Putative effectors also include F-box adaptor proteins that may re-target host ubiquitylation systems, may function to de-SUMOylate transcription factors, and may inhibit proteasome activities.[19,20] CHS3/DAR4 LP domain protein levels were not affected by AcEm2 infection (Figure S7), and DAR4 showed relatively a low efficiency of inhibition to DA1 peptidase activity (Figure 7E). This suggests DAR4 originally served as a paralogous decoy to guard DAR3 and subsequently integrated into the NLR protein CHS3/DAR4 to serve as an integrated decoy during *Brassicaceae* evolution.

STAR★METHODS

Detailed methods are provided in the online version of this paper and include the following:

- KEY RESOURCES TABLE
- RESOURCE AVAILABILITY
  - Lead contact
  - Materials availability
  - Data and code availability
- EXPERIMENTAL MODEL AND SUBJECT DETAILS
  - Arabidopsis thaliana
  - Nicotiana tabacum
  - Bacterial strains
- METHOD DETAILS
  - Plasmid constructions
  - *Agrobacterium*-Mediated Transient Transformation of *N. tabacum* and HR assays
  - Protein expression in *Arabidopsis* protoplasts
  - DA1 domain swap *in vitro* ubiquitination test
  - Pathogen growth tests
  - Protein extraction and analyses
  - Protein co-immunoprecipitation
  - Ploidy levels
  - Nucleotide diversity of *DA1* and *DAR3*
  - Phylogenetic analysis
- QUANTIFICATION AND STATISTICAL ANALYSIS

SUPPLEMENTAL INFORMATION

Supplemental information can be found online at https://doi.org/10.1016/j.chom.2023.04.009.

ACKNOWLEDGMENTS

We thank Dr. Yan Ma for advice on *N. tabacum* infiltration, and Drs. Catherine Gardener, Dae Sung Kim, Xiaokun Liu, and Pingtao Ding for advice on pathogen growth tests. This work was funded by the Biological and Biotechnological Sciences Research Council (BBSRC) Newton Fund to B.G. and M.W.B., BBSRC grant BB/K017225 to M.W.B., and Institute Strategic Grant GEN (BB/P013511/1) to M.W.B. Work in the J.D.G.J. lab was supported by a Gatsby Charitable Foundation grant to TSL Norwich, by BBSRC BB/M003809/1 (supported V.C.) and ERC grant 233376 "Albugon" (supported VK). Work in the V.C. lab was supported by the University of Bath University Research Studentship Account (URSA), University of Bath start-up fund, and Royal Society International Collaboration Awards (ICA\R1\201511). We thank the 1001 Genomes Plus (1001G+) project, funded by ERA-CAPS through BBSRC, DFG, and FWF to Paul Kersey, Detlef Weigel, and Magnus Nordborg, for access to newly assembled *Arabidopsis* genomes.

AUTHOR CONTRIBUTIONS

B.G., V.C., J.D.G.J., D.W., and M.W.B. designed the research. B.G., T.P., F.R., C.S., F.H.-L., H.D., and N.M. performed experiments, B.G. and F.R. analyzed data, and M.W.B., B.G., and J.D.G.J. wrote the manuscript.

DECLARATION OF INTERESTS

The authors declare no competing interests.

Received: July 17, 2022
Revised: March 9, 2023
Accepted: April 6, 2023
Published: May 10, 2023

REFERENCES

1. Barbetti, M.J., Li, C.X., You, M.P., Singh, D., Agnihotri, A., Banga, S.K., Sandhu, P.S., Singh, R., and Banga, S.S. (2016). Valuable new leaf or inflorescence resistances ensure improved management of white rust (Albugo candida) in mustard (Brassica juncea) crops. J. Phytopathol. *164*, 404–411. https://doi.org/10.1111/jph.12425.
2. Arora, H., Padmaja, K.L., Paritosh, K., Mukhi, N., Tewari, A.K., Mukhopadhyay, A., Gupta, V., Pradhan, A.K., and Pental, D. (2019). BjuWRR1, a CC-NB-LRR gene identified in Brassica juncea, confers resistance to white rust caused by Albugo candida. Theor. Appl. Genet. *132*, 2223–2236. https://doi.org/10.1007/s00122-019-03350-z.
3. Bhayana, L., Paritosh, K., Arora, H., Yadava, S.K., Singh, P., Nandan, D., Mukhopadhyay, A., Gupta, V., Pradhan, A.K., and Pental, D. (2019). A mapped locus on LG A6 of Brassica juncea Line Tumida conferring resistance to white rust contains a CNL Type R gene. Front. Plant Sci. *10*, 1690. https://doi.org/10.3389/fpls.2019.01690.
4. Parkes, T. (2020). From Recognition to Susceptibility: Functional characterisation of plant-specific LIM-domain containing proteins in plant-microbe interactions. PhD Thesis (University of Bristol).
5. Yang, Y., Kim, N.H., Cevik, V., Jacob, P., Wan, L., Furzer, O.J., and Dangl, J.L. (2022). Allelic variation in the Arabidopsis TNL CHS3/CSA1 immune receptor pair reveals two functional regulatory modes. Cell Host Microbe *30*, 1701–1716.e5. https://doi.org/10.1016/j.chom.2022.09.013.
6. Cevik, V., Boutrot, F., Apel, W., Robert-Seilaniantz, A., Furzer, O.J., Redkar, A., Castel, B., Kover, P.X., Prince, D.C., Holub, E.B., and Jones, J.D.G. (2019). Transgressive segregation reveals mechanisms of Arabidopsis immunity to Brassica-infecting races of white rust (Albugo candida). Proc. Natl. Acad. Sci. USA *116*, 2767–2773. https://doi.org/10.1073/pnas.1812911116.
7. Redkar, A., Cevik, V., Bailey, K., Zhao, H., Kim, D.S., Zou, Z., Furzer, O.J., Fairhead, S., Borhan, M.H., Holub, E.B., and Jones, J.D.G. (2023). The Arabidopsis WRR4A and WRR4B paralogous NLR proteins both confer recognition of multiple Albugo candida effectors. New Phytol. *237*, 532–547. https://doi.org/10.1111/nph.18378.
8. Zhu, C., Holub, E.B., Xu, F., Jones, J.D., Johnson, K., Sohn, K., Cevik, V., Li, X., and Liu, Y. (2015). Autoimmunity conferred by *chs3-2D* relies on *CSA1*, its adjacent TNL-encoding neighbour. Sci. Rep. *5*, 8792. https://doi.org/10.1038/srep08792.
9. Sarris, P.F., Duxbury, Z., Huh, S.U., Ma, Y., Segonzac, C., Sklenar, J., Derbyshire, P., Cevik, V., Rallapalli, G., Saucet, S.B., et al. (2015). A plant immune receptor detects pathogen effectors that target WRKY transcription factors. Cell *161*, 1089–1100. https://doi.org/10.1016/j.cell.2015.04.024.

10. Sarris, P.F., Cevik, V., Dagdas, G., Jones, J.D.G., and Krasileva, K.V. (2016). Comparative analysis of plant immune receptor architectures uncovers host proteins likely targeted by pathogens. BMC Biol. *14*, 8. https://doi.org/10.1186/s12915-016-0228-7.

11. Kroj, T., Chanclud, E., Michel-Romiti, C., Grand, X., and Morel, J.B. (2016). Integration of decoy domains derived from protein targets of pathogen effectors into plant immune receptors is widespread. New Phytol. *210*, 618–626. https://doi.org/10.1111/nph.13869.

12. Schulze, S., Yu, L., Hua, C., Zhang, L., Kolb, D., Weber, H., Ehinger, A., Saile, S.C., Stahl, M., Franz-Wachtel, M., et al. (2022). The Arabidopsis TIR-NBS-LRR protein CSA1 guards BAK1-BIR3 homeostasis and mediates convergence of pattern- and effector-induced immune responses. Cell Host Microbe *30*, 1717–1731.e6. https://doi.org/10.1016/j.chom.2022.11.001.

13. Cesari, S., Bernoux, M., Moncuquet, P., Kroj, T., and Dodds, P.N. (2014). A novel conserved mechanism for plant NLR protein pairs: the "integrated decoy" hypothesis. Front. Plant Sci. *5*, 606. https://doi.org/10.3389/fpls.2014.00606.

14. Ortiz, D., de Guillen, K., Cesari, S., Chalvon, V., Gracy, J., Padilla, A., and Kroj, T. (2017). Recognition of the Magnaporthe oryzae effector AVR-pia by the decoy domain of the rice NLR immune receptor RGA5. Plant Cell *29*, 156–168. https://doi.org/10.1105/tpc.16.00435.

15. Białas, A., Langner, T., Harant, A., Contreras, M.P., Stevenson, C.E., Lawson, D.M., Sklenar, J., Kellner, R., Moscou, M.J., Terauchi, R., et al. (2021). Two NLR immune receptors acquired high-affinity binding to a fungal effector through convergent evolution of their integrated domain. eLife *10*. https://doi.org/10.7554/eLife.66961.

16. van der Hoorn, R.A.L., and Kamoun, S. (2008). From Guard to Decoy: a new model for perception of plant pathogen effectors. Plant Cell *20*, 2009–2017. https://doi.org/10.1105/tpc.108.060194.

17. Weßling, R., Epple, P., Altmann, S., He, Y., Yang, L., Henz, S.R., McDonald, N., Wiley, K., Bader, K.C., Gläßer, C., et al. (2014). Convergent targeting of a common host protein-network by pathogen effectors from three kingdoms of life. Cell Host Microbe *16*, 364–375. https://doi.org/10.1016/j.chom.2014.08.004.

18. Jones, J.D.G., Vance, R.E., and Dangl, J.L. (2016). Intracellular innate immune surveillance devices in plants and animals. Science *354*, aaf6395. https://doi.org/10.1126/science.aaf6395.

19. Mukhi, N., Gorenkin, D., and Banfield, M.J. (2020). Exploring folds, evolution and host interactions: understanding effector structure/function in disease and immunity. New Phytol. *227*, 326–333. https://doi.org/10.1111/nph.16563.

20. Franceschetti, M., Maqbool, A., Jiménez-Dalmaroni, M.J., Pennington, H.G., Kamoun, S., and Banfield, M.J. (2017). Effectors of filamentous plant pathogens: commonalities amid diversity. Microbiol. Mol. Biol. Rev. *81*. https://doi.org/10.1128/MMBR.00066-16.

21. Li, Y., Zheng, L., Corke, F., Smith, C., and Bevan, M.W. (2008). Control of final seed and organ size by the DA1 gene family in Arabidopsis thaliana. Genes Dev. *22*, 1331–1336. https://doi.org/10.1101/gad.463608.

22. Bach, I. (2000). The LIM domain: regulation by association. Mech. Dev. *91*, 5–17.

23. Dong, H., Dumenil, J., Lu, F.H., Na, L., Vanhaeren, H., Naumann, C., Klecker, M., Prior, R., Smith, C., McKenzie, N., et al. (2017). Ubiquitylation activates a peptidase that promotes cleavage and destabilization of its activating E3 ligases and diverse growth regulatory proteins to limit cell proliferation in Arabidopsis. Genes Dev. *31*, 197–208. https://doi.org/10.1101/gad.292235.116.

24. Gu, B., Dong, H., Smith, C., Cui, G., Li, Y., and Bevan, M.W. (2022). Modulation of receptor-like trans-membrane kinase 1 nuclear localisation by DA1 peptidases in Arabidopsis. Proc. Natl. Acad. Sci. USA *119*. e2205757119. https://doi.org/10.1073/pnas.2205757119.

25. Van de Weyer, A.L., Monteiro, F., Furzer, O.J., Nishimura, M.T., Cevik, V., Witek, K., Jones, J.D.G., Dangl, J.L., Weigel, D., and Bemm, F. (2019). A species-wide inventory of NLR genes and alleles in Arabidopsis thaliana. Cell *178*, 1260–1272.e14. https://doi.org/10.1016/j.cell.2019.07.038.

26. Zhou, J.M., and Zhang, Y. (2020). Plant immunity: danger perception and signaling. Cell *181*, 978–989. https://doi.org/10.1016/j.cell.2020.04.028.

27. Dong, H., Smith, C., Prior, R., Carter, R., Dumenil, J., Saalbach, G., McKenzie, N., and Bevan, M. (2020). The receptor kinase BRI1 promotes cell proliferation in Arabidopsis by phosphorylation- mediated inhibition of the growth repressing peptidase DA1. https://doi.org/10.1101/2020.05.15.098178.

28. Yang, H., Shi, Y., Liu, J., Guo, L., Zhang, X., and Yang, S. (2010). A mutant CHS3 protein with TIR-NB-LRR-LIM domains modulates growth, cell death and freezing tolerance in a temperature-dependent manner in Arabidopsis. Plant J. *63*, 283–296. https://doi.org/10.1111/j.1365-313X.2010.04241.x.

29. Ma, Y., Guo, H., Hu, L., Martinez, P.P., Moschou, P.N., Cevik, V., Ding, P., Duxbury, Z., Sarris, P.F., and Jones, J.D.G. (2018). Distinct modes of derepression of an Arabidopsis immune receptor complex by two different bacterial effectors. Proc. Natl. Acad. Sci. USA *115*, 10218–10227. https://doi.org/10.1073/pnas.1811858115.

30. Bailey, P.C., Schudoma, C., Jackson, W., Baggs, E., Dagdas, G., Haerty, W., Moscou, M., and Krasileva, K.V. (2018). Dominant integration locus drives continuous diversification of plant immune receptors with exogenous domain fusions. Genome Biol. *19*, 23. https://doi.org/10.1186/s13059-018-1392-6.

31. Le Roux, C., Huet, G., Jauneau, A., Camborde, L., Trémousaygue, D., Kraut, A., Zhou, B., Levaillant, M., Adachi, H., Yoshioka, H., et al. (2015). A receptor pair with an integrated decoy converts pathogen disabling of transcription factors to immunity. Cell *161*, 1074–1088. https://doi.org/10.1016/j.cell.2015.04.025.

32. Peng, Y., Chen, L., Lu, Y., Wu, Y., Dumenil, J., Zhu, Z., Bevan, M.W., and Li, Y. (2015). The ubiquitin receptors DA1, DAR1, and DAR2 redundantly regulate endoreduplication by modulating the stability of TCP14/15 in Arabidopsis. Plant Cell *27*, 649–662. https://doi.org/10.1105/tpc.114.132274.

33. Du, L., Li, N., Chen, L., Xu, Y., Li, Y., Zhang, Y., Li, C., and Li, Y. (2014). The ubiquitin receptor DA1 regulates seed and organ size by modulating the stability of the ubiquitin-specific protease UBP15/SOD2 in Arabidopsis. Plant Cell *26*, 665–677. https://doi.org/10.1105/tpc.114.122663.

34. Chandran, D., Rickert, J., Cherk, C., Dotson, B.R., and Wildermuth, M.C. (2013). Host cell ploidy underlying the fungal feeding site is a determinant of powdery mildew growth and reproduction. Mol. Plant Microbe Interact. *26*, 537–545. https://doi.org/10.1094/MPMI-10-12-0254-R.

35. Hamdoun, S., Liu, Z., Gill, M., Yao, N., and Lu, H. (2013). Dynamics of defense responses and cell fate change during Arabidopsis-Pseudomonas syringae interactions. PLoS One *8*, e83219. https://doi.org/10.1371/journal.pone.0083219.

36. Wildermuth, M.C., Steinwand, M.A., McRae, A.G., Jaenisch, J., and Chandran, D. (2017). Adapted biotroph manipulation of plant cell ploidy. Annu. Rev. Phytopathol. *55*, 537–564. https://doi.org/10.1146/annurev-phyto-080516-035458.

37. Yang, Y., Kim, N.H., Cevik, V., Jacob, P., Wan, L., Furzer, O.J., and Dangl, J.L. (2022). Allelic variation in the Arabidopsis TNL CHS3/CSA1 immune receptor pair reveals two functional cell-death regulatory modes. Cell Host Microbe *30*, 1701–1716.e5. https://doi.org/10.1016/j.chom.2022.09.013.

38. Tajima, F. (1989). Statistical method for testing the neutral mutation hypothesis by DNA polymorphism. Genetics *123*, 585–595.

39. Bi, D., Johnson, K.C.M., Zhu, Z., Huang, Y., Chen, F., Zhang, Y., and Li, X. (2011). Mutations in an atypical TIR-NB-LRR-LIM resistance protein confer autoimmunity. Front. Plant Sci. *2*, 71. https://doi.org/10.3389/fpls.2011.00071.

40. Zhang, N., Wang, Z., Bao, Z., Yang, L., Wu, D., Shu, X., and Hua, J. (2018). MOS1 functions closely with TCP transcription factors to modulate immunity and cell cycle in Arabidopsis. Plant J. *93*, 66–78. https://doi.org/10.1111/tpj.13757.

41. Banfield, M.J. (2015). Perturbation of host ubiquitin systems by plant pathogen/pest effector proteins. Cell. Microbiol. *17*, 18–25. https://doi.org/10.1111/cmi.12385.

42. Cuppels, D.A. (1986). Generation and Characterization of Tn5 Insertion Mutations in Pseudomonas syringae pv. tomato. Appl. Environ. Microbiol. *51*, 323–327.51.

43. McMullan, M., Gardiner, A., Bailey, K., Kemen, E., Ward, B.J., Cevik, V., Robert-Seilaniantz, A., Schultz-Larsen, T., Balmuth, A., Holub, E., et al. (2015). Evidence for suppression of immunity as a driver for genomic introgressions and host range expansion in races of Albugo candida, a generalist parasite. Elife *4*. https://doi.org/10.7554/eLife.04550.

44. Vanhaeren, H., Nam, Y.J., De Milde, L., Chae, E., Storme, V., Weigel, D., Gonzalez, N., and Inzé, D. (2017). Forever young: the role of ubiquitin receptor DA1 and E3 ligase BIG BROTHER in controlling leaf growth and development. Plant Physiol. *173*, 1269–1282. https://doi.org/10.1104/pp.16.01410.

45. Ruhe, J., Agler, M.T., Placzek, A., Kramer, K., Finkemeier, I., and Kemen, E.M. (2016). Obligate biotroph pathogens of the genus Albugo Are Better adapted to active Host Defense Compared to Niche Competitors. Front. Plant Sci. *7*, 820. https://doi.org/10.3389/fpls.2016.00820.

46. Hanušová, K., Ekrt, L., Vít, P., Kolář, F., and Urfus, T. (2014). Continuous morphological variation correlated with genome size indicates frequent introgressive hybridization among Diphasiastrum species (Lycopodiaceae) in Central Europe. PLoS One *9*, e99552. https://doi.org/10.1371/journal.pone.0099552.

47. Koren, S., Walenz, B.P., Berlin, K., Miller, J.R., Bergman, N.H., and Phillippy, A.M. (2017). Canu: scalable and accurate long-read assembly via adaptive k-mer weighting and repeat separation. Genome Res. *27*, 722–736. https://doi.org/10.1101/gr.215087.116.

48. Shumate, A., and Salzberg, S.L. (2020). Liftoff: accurate mapping of gene annotations. Bioinformatics *37*, 1639–1643. https://doi.org/10.1093/bioinformatics/btaa1016.

49. Li, H., Handsaker, B., Wysoker, A., Fennell, T., Ruan, J., Homer, N., Marth, G., Abecasis, G., and Durbin, R.; 1000 Genome Project Data Processing Subgroup (2009). The Sequence Alignment/Map format and SAMtools. Bioinformatics *25*, 2078–2079. https://doi.org/10.1093/bioinformatics/btp352.

50. Pertea, G., and Pertea, M. (2020). GFF Utilities: GffRead and GffCompare. F1000Res *9*, 304. https://doi.org/10.12688/f1000research.23297.2.

51. Katoh, K., and Standley, D.M. (2013). MAFFT multiple sequence alignment software version 7: improvements in performance and usability. Mol. Biol. Evol. *30*, 772–780. https://doi.org/10.1093/molbev/mst010.

52. Paradis, E., and Schliep, K. (2019). ape 5.0: an environment for modern phylogenetics and evolutionary analyses in R. Bioinformatics *35*, 526–528. https://doi.org/10.1093/bioinformatics/bty633.

53. Paradis, E. (2010). pegas: an R package for population genetics with an integrated-modular approach. Bioinformatics *26*, 419–420. https://doi.org/10.1093/bioinformatics/btp696.

54. Edgar, R.C. (2004). MUSCLE: a multiple sequence alignment method with reduced time and space complexity. BMC Bioinformatics *5*, 113. https://doi.org/10.1186/1471-2105-5-113.

Please cite this article in press as: Gu et al., The integrated LIM-peptidase domain of the CSA1-CHS3/DAR4 paired immune receptor detects changes in DA1 peptidase inhibitors in *Arabidopsis*, Cell Host & Microbe (2023), https://doi.org/10.1016/j.chom.2023.04.009

STAR★METHODS

KEY RESOURCES TABLE

REAGENT or RESOURCE	SOURCE	IDENTIFIER
Antibodies		
Mouse monoclonal ANTI-FLAG® M2-Peroxidase (HRP) antibody	Sigma	Cat#A8592, RRID:AB_439702
Mouse monoclonal GFP Antibody, HRP	MiltenyiBiotec	Cat#130-091-833
Rat clone 3F10, monoclonal anti-HA-Peroxidase, High Affinity	Roche	Cat#12013819001 RRID:AB_390917
Mouse monoclonal Anti-α-Tubulin antibody	Sigma	Cat#T5168 RRID:AB_477579
Goat polyclonal anti-Rabbit IgG (whole molecule)–Peroxidase antibody	Sigma	Cat#A0545 RRID:AB_257896
Bacterial and virus strains		
Pseudomonas syringae pv *tomato* (Pst) DC3000	Davis et al.[42]	N/A
Albugo candida AcEM2	McMullan et al.[43]	N/A
Agrobacterium tumefaciens strain GV3101	Gold Biotechnology	Cat#CC-207-5x50
Escherichia coli DH5α	Thermofisher	Cat#18258012
Escherichia coli BL21	TransGen Biotech	Cat#CD901-03
Chemicals, peptides, and recombinant proteins		
$MgCl_2.6H_2O$	Sigma	Cat#1374248
MES hydrate	Sigma	Cat#M2933
Isopropyl β- d-1-thiogalactopyranoside (IPTG)	Sigma	Cat#I6758
HEPES	Sigma	Cat#H3375
KOH	Sigma	Cat#Z422312
NaCl	Sigma	Cat#S9888
Glycerol	Sigma	Cat#G5516
Triton X-100	Sigma	Cat#X100
EDTA-free protease inhibitor cocktail	Roche	Cat#10103D
E1 (Human UBE1)	Boston Biochem	Cat#E-308-050
E2 (Human UbcH5b/UBE2D2)	Boston Biochem	Cat#E2-622-100
Ubiquitin	Boston Biochem	Cat#U-100H
Anti-HA magnetic beads	ThermoFisher	Cat#Cat#88836
NP-40	Sigma	Cat#492016
Citric acid	Sigma	Cat#251275
Tween20	Sigma	Cat#P1379
$Na_2HPO_4.12H_2O$	Sigma	Cat#1.06573
β-mercaptoethanol	Sigma	Cat#M6250
Propidium Iodide (PI)	Sigma	Cat#P4864
RNase IIA	Sigma	Cat#R5000

(*Continued on next page*)

Please cite this article in press as: Gu et al., The integrated LIM-peptidase domain of the CSA1-CHS3/DAR4 paired immune receptor detects changes in DA1 peptidase inhibitors in *Arabidopsis*, Cell Host & Microbe (2023), https://doi.org/10.1016/j.chom.2023.04.009

Continued

REAGENT or RESOURCE	SOURCE	IDENTIFIER
MG132(Z-Leu-Leu-Leu-al)	Sigma	Cat#C2211
Dynabeads™ His-Tag Isolation and Pulldown	ThermoFisher	Cat# 10103D
Critical commercial assays		
In-Fusion® HD Cloning Plus	Takara	Cat#638909
pENTR™/D-TOPO® Gateway	ThermoFisher	Cat#K243520
pDONR207 Gateway	Takara	Cat#638909
Gateway™ LR Clonase™ II Enzyme	Invitrogen	Cat#11791-020
LIGHTCYCLER 480 SYBR GREEN I MASTER MIX	Roche	Cat#04707516001
Deposited data		
De novo assemblies of *CHS3/DAR4*	GenBank	OQ505065–OQ505090
De novo assemblies of *DA1*	GenBank	OQ505011–OQ505037
De novo assemblies of *DAR3*	GenBank	OQ505038–OQ505064
Experimental models: Organisms/strains		
Arabidopsis thaliana Col-0		
da1-ko1dar1-1	Dong et al.[23]	N/A
da1ko1	Dong et al.[23]	SALK_126092
dar1-1	Dong et al.[23]	SALK_067100
dar3-1	This paper	SAIL_15_D09
dar3-2	This paper	N/A
dar3-3	This paper	N/A
35S::DA1-GFP ox-DA1-1.3	Vanhaeren et al.[44]	N/A
35S::DA1-GFP ox-DA1-1.4-13	Vanhaeren et al.[44]	N/A
Arabidopsis thaliana Ws-2		
da1ko1dar1-1	This paper	N/A
35S::3HA-DA1-Ws-2_1	This paper	N/A
35S::DA1-GFP_Ws-2_1	This paper	N/A
35S::DA1-GFP_Ws-2_2	This paper	N/A
3SS::3HA-DAR3-Ws-2_1	This paper	N/A
35S::DAR3-GFP_Ws-2_1	This paper	N/A
35S::DAR3-GFP_Ws-2_2	This paper	N/A
35S::3HA-DAR4$^{aa1127\text{-}1613}$-Ws-2_1	This paper	N/A
Oligonucleotides		
Primers see Table S12	Sigma	Custom order
Recombinant DNA		
pETnT	Dong et al.[23]	N/A
pAGM4723_ccdB	Synbio	https://synbio.tsl.ac.uk
35S::BB-3FLAG	Dong et al.[23]	N/A
35S::3HA-DA1	Dong et al.[23]	Addgene 190758
35S::3HA-DAR1	Dong et al.[23]	Addgene 190760
35S::3HA-DAR2	Dong et al.[23]	Addgene 190761
35S::3HA-DAR4	This paper	Addgene 200562
35S::3HA-chs3-1	This paper	Addgene 200563
35S::3HA-chs3-2d	This paper	Addgene 200564
35S::3HA-dar4p1037	This paper	Addgene 200565
35S::3HA-dar4p1237	This paper	Addgene 200566

(*Continued on next page*)

Continued

REAGENT or RESOURCE	SOURCE	IDENTIFIER
35S::3HA-dar4-pep	This paper	Addgene 200567
35S::3HA-dar4-EEII	This paper	Addgene 200568
35S::3HA-dar4-LP(GST)	This paper	Addgene 200569
35S::3HA-dar4-LP(GFP)	This paper	Addgene 200570
35S::3HA-DAR4-LP(DA1)	This paper	Addgene 200571
35S::3HA-DAR4-LP(DA1)-2d	This paper	Addgene 200572
35S::3HA-DAR4-LP(DAR1)	This paper	Addgene 200573
35S::3HA-DAR4-LP(DAR2)	This paper	Addgene 200574
35S::3HA-DAR4-LP(DAR3)	This paper	Addgene 200575
35S::3HA-DAR4-LP(DAR5)	This paper	Addgene 200576
35S::3HA-DAR4-LP(DAR6)	This paper	Addgene 200577
35S::3HA-DAR4-LP(DAR7)	This paper	Addgene 200578
35S::3HA-da1-pep	Dong et al.[23]	Addgene 190759
35S::3HA-da1-L(DAR4)	This paper	Addgene 200579
35S::3HA-da1-L1(DAR4)	This paper	Addgene 200580
35S::3HA-da1-L2(DAR4)	This paper	Addgene 200581
35S::3HA-da1-L3(DAR4)	This paper	Addgene 200582
35S::3HA-da1-L4(DAR4)	This paper	Addgene 200583
35S::3HA-da1-P(DAR4)	This paper	Addgene 200584
35S::3HA-da1-P1(DAR4)	This paper	Addgene 200585
35S::3HA-da1-P2(DAR4)	This paper	Addgene 200586
35S::3HA-da1-P3(DAR4)	This paper	Addgene 200587
35S::3HA-da1-P2+3(DAR4)	This paper	Addgene 200588
35S::3HA-da1-LP(DAR4)	This paper	Addgene 200589
35S::DA1-GFP	This paper	Addgene 200590
35S::BB-3FLAG	Dong et al.[23]	N/A
35S::DAR3-GFP	This paper	Addgene 200591
35S::DAR7-GFP	This paper	Addgene 200592
35S::dar3-LP(DA1)-GFP	This paper	Addgene 200593
35S::dar3-LP(DAR4)-GFP	This paper	Addgene 200594
35S::DAR4 $^{aa1127\text{-}1613}$*-GFP*	This paper	Addgene 200595
35S::3HA-DAR4 $^{aa1127\text{-}1613}$	This paper	Addgene 200596
35S::3HA-DAR3	This paper	Addgene 200597
35S::DA1-3FLAG	Dong et al.[23]	N/A
35S::DAR1-3FLAG	This paper	Addgene 200598
35S::DAR2-3FLAG	This paper	Addgene 200599
35S::DAR3-3FLAG	This paper	Addgene 200600
35S::GFP	Dong et al.[23]	Addgene 200600
35S::TIR(CSA1)-GFP	This paper	Addgene 200601
35S::TIR(DAR4)-GFP	This paper	Addgene 200602
DA1-pETnT	Dong et al.[23]	N/A
da1-LP(DAR4)-pETnT	This paper	Addgene 200603
da1-L(DAR4)-pETnT	This paper	Addgene 200604
da1-P(DAR4)-pETnT	This paper	Addgene 200605
DA2-pET24a	Dong et al.[23]	N/A
Software and algorithms		
MEGA-X	Version X	https://www.megasoftware.net/

Please cite this article in press as: Gu et al., The integrated LIM-peptidase domain of the CSA1-CHS3/DAR4 paired immune receptor detects changes in DA1 peptidase inhibitors in *Arabidopsis*, Cell Host & Microbe (2023), https://doi.org/10.1016/j.chom.2023.04.009

RESOURCE AVAILABILITY

Lead contact

Further information and requests for resources and reagents should be directed to and will be fulfilled by the lead contact Michael Bevan (michael.bevan@jic.ac.uk)

Materials availability

There are no restrictions on the availability of materials. Plasmids generated in this study are available from Addgene. Transgenic lines are available from the lead contact.

Data and code availability

- Sequences of *CSA1, CHS3/DAR4, DA1* and *DAR3* are publicly available from Genbank. Accession numbers are listed in the key resources table. All data generated in this study are in Tables S1–S16.
- No original code was used in this study.
- Any additional information required to re-analyze the data reported in this paper is available from the lead contact upon request.

EXPERIMENTAL MODEL AND SUBJECT DETAILS

Arabidopsis thaliana

Arabidopsis thaliana Col-0 and Ws-2 plants were grown in short days (10 hours light/ 14 hours dark) at 20°C. Ws-2 was crossed with the Col-0 *da1-ko1dar1-1* double mutant and backcross lines were selected in the BC7F2 population using primers in Table S13 to genotype *DA1* and *DAR1* genes.

Nicotiana tabacum

Nicotiana tabacum plants were grown in long days (16 hours light/ 8 hours dark) at 24°C.

Bacterial strains

Escherichia coli was grown at 37°C in Luria Broth with antibiotics as described

Agrobacterium tumefaciens was grown at 28°C in Luria Broth with antibiotics as described.

METHOD DETAILS

Plasmid constructions

Coding sequences of genes were amplified and ligated into pENTR™/D-TOPO® (ThermoFisher, Catalog number K243520) or pDONR207 by in-fusion (Takara, Catalog Number 638909), then transferred into expression plasmids by LR reactions (Invitrogen, Catalog Number 11791-020). For protein expression in *Escherichia coli* coding sequences were ligated into pETnT by in-fusion.[23] Site mutation and domain swapped constructs were amplified by PCR and ligated by in-fusion. DAR3 guide RNAs were assembled using GoldenGate into pAGM4723_ccdB using FastRed selection. This selection gene was removed after genotyping by backcrossing with wild type Ws-2. Expression plasmids are described in Table S14. Table S15 shows mutant lines used. Transgenic lines used are shown in Table S16. DA1-GFP over- expression lines are from Vanhaeren et al.[44]

Agrobacterium-Mediated Transient Transformation of *N. tabacum* and HR assays

Agrobacterium GV3101 strains were grown in LB-medium overnight supplemented with appropriate antibiotics. Cells were harvested and adjusted to OD600 0.5 in resuspension buffer (10 mM $MgCl_2$, 10 mM MES pH 5.6), then infiltrated into 4 to 5 weeks old *N. tabacum* leaves.[9] HR reactions were scored after 2 to 3 days according to Ma et al.[29]

Protein expression in *Arabidopsis* protoplasts

BB cleavage was assessed by co-expressing 35S::BB-3FLAG with 35S::3HA-DA1 and mutant variants in *da1-ko1dar1-1* leaf protoplasts.[9,23] Expression levels of CSA1, DAR4 and mutant variants were assessed in Ws-2 leaf protoplasts. DAR3 inhibition of DA1 was tested in *da1-ko1dar1-1* leaf protoplast cells using a concentration of 50,000 cells/200 μl and 10 μg of purified plasmid DNA.

DA1 domain swap *in vitro* ubiquitination test

DA1 domain swap proteins were expressed in *E. coli* BL21 (DE3) as C-terminal HIS-tagged proteins. Cells were grown to OD600 0.6 in LB-medium at 37°C, and induced by 0.1mM Isopropyl β- d-1-thiogalactopyranoside (IPTG) for 3 hours at 28°C. Cells were harvested, disrupted by sonication (4 x 5 sec bursts with 20 sec interval) in TGH buffer (50 mM HEPES-KOH pH 7.4, 150 mM NaCl, 10% (v/v) glycerol, 1% (v/v) Triton X-100, with EDTA-free protease inhibitor cocktail (Roche Catalog number 11873580001)) and purified by Dynabeads™ His-Tag Isolation and Pulldown (ThermoFisher, Catalog number 10103D). Ubiquitylation reactions used E1 (Human UBE1, Boston Biochem, Catalog number E-308-050), E2 (Human UbcH5b/UBE2D2, Boston Biochem, Catalog number E2-622-100), E3

(purified DA2) with ubiquitin (Boston Biochem, Catalog number U-100H) in reaction buffer at 30ºC for 8 hours *in vitro* according to Dong et al.[23] Protein ubiquitination was tested by immunoblots and FLAG-HRP antibody (Sigma, Catalog number A8592).

Pathogen growth tests

Pseudomonas syringae Pst DC3000 at an OD600 0.02 were sprayed onto 17 day old *Arabidopsis* seedlings and plants were harvested 40 hours after inoculation.[9,23] Leaves were sterilised in 75% ethanol for 15 seconds, washed in water for 1 min and weighed before maceration in 10 mM $MgCl_2$. Serial dilutions were plated and grown at 28°C for 2 days and colony-forming units were counted. *Hpa* Noco2 spores were sprayed onto 14-day-Arabidopsis seedlings at a concentration of 10,000 spores/ml, then grown at 16ºC for 7 to 10 days. Spores were washed from plants and concentrations were calculated using a cytometer. *A. candida* Ac Em2 spores (10^5 /ml or 10^4 /ml) were sprayed on 4 to 5 week-old plants that were grown in short day conditions for 10 days. Pathogen growth was measured by quantitative PCR using LIGHTCYCLER 480 SYBR GREEN MASTER MIX (Roche, Catalog number 04707516001) to measure ratios of host genomic DNA to pathogen DNA ITS (pathogen)/EF1-α (host).[45]

Protein extraction and analyses

Total protein was extracted in 10 mM Tris HCl pH 7.5, 150 mM NaCl, 0.5 mM EDTA, 10% Glycerol, 0.5% NP-40, EDTA-free Protease Inhibitor Cocktail. DAR3-GFP levels were assessed using immunoblots with GFP antibody (MiltenyiBiotec, Anti-GFP-HRP, Catalog number 130-091-833), 3HA-DA1, 3HA-DAR3 and 3HA-DAR4$^{aa127\text{-}1613}$ by HA-HRP (Sigma, Catalog number 12013819001) and αTubulin levels were used as loading control (α-Tubulin antibody, Monoclonal mouse Anti-α-Tubulin antibody, Sigma, Catalog number T5168; anti-Rabbit IgG, Sigma, Catalog number A0545).

Protein co-immunoprecipitation

3HA-DAR3 and DA1 family proteins tagged with 3FLAG were expressed in Arabidopsis *da1-ko1dar1-1* leaf protoplast cells. Proteins were extracted and purified using Pierce Anti-HA magnetic beads (ThermoFisher Catalog number 88836) for 3 hours. After 4 washes in 10 mM TrisHCl pH 7.5, 150 mM NaCl, 10% Glycerol, 0.5% NP-40, EDTA-free Protease Inhibitor Cocktail, bound proteins were eluted at 95ºC for 5 minutes in 1 x SDS sample buffer. Protein levels were assessed using immunoblots with HA-HRP (Sigma, Catalog number 12013819001) or FLAG-HRP antibodies (Sigma, Catalog number A8592).

Ploidy levels

Three 5mm leaf discs from one Arabidopsis plant were chopped in Otto buffer I (0.1 M citric acid, 0.5% Tween 20), passed through a 30 μm filter, diluted with 2 volumes of Otto buffer II (0.4 M $Na_2HPO_4 \cdot 12\ H_2O$, 2μl/ml β-mercaptoethanol, 50 μg/ml propidium iodide (PI) and 50 μg/ml RNase IIA) and kept at room temperature for 5 min. Ploidy levels were measured using a BD FACSMelody™ Cell Sorter.[46] The ploidy index was calculated as (% 4C nuclei x 1) + (% 8C nuclei x 2) + (% 16C nuclei x 3) + (% 32C nuclei x 4) + (% 64C nuclei x 5).

Nucleotide diversity of *DA1* and *DAR3*

Long-read-based assemblies of 27 diverse *A. thaliana* accessions were from the 1001 Genome Plus project. These genomes were sequenced with PacBio Continuous Long Reads (CLRs), assembled with Canu (version 1.71),[47] and polished with long-reads and PCR-free short-reads. Protein coding genes were annotated with Liftoff (version 1.6.2),[48] using the annotation file 'Araport11_GFF3_genes_transposons.201606.gff' downloaded from https://www.arabidopsis.org. Loci corresponding to genes *AT5G17880-AT5G17890* (*CSA1-CHS3/DAR4*), *AT1G19270* (*DA1*), *AT5G66610* and *AT5G66640* (*DAR7* and *DAR3*) plus 3 kb flanking sequence were extracted with 'samtools faidx' (version 1.9).[49] Coding DNA Sequences (CDS) of *DA1* and *DAR3* were extracted with gffread (version 0.12.7).[50] *CHS3/DAR4* was manually annotated due to the high variability of the LIM-peptidase ID. Accessions were classified according to the presence (clade 1; 13 accessions) or absence (clade 2; 12 accessions) of the LIM-peptidase ID in the *CHS3/DAR4* gene. Multiple alignments of the CDS of genes *DA1* and *DAR3* were performed separately for sets of accessions corresponding to each clade with MAFFT (version 7.407; –reorder –maxiterate 1000 –retree 1).[51] Nucleotide diversity and Tajima's D were estimated from the aligned sequences with R-packages ape (version 5.6.2)[52] and pegas (version 1.1).[53] These estimates were compared with those obtained in 5,000 random combinations of 12 or 13 accessions drawn from 25 eligible accessions of the genes *DA1* and *DAR3* (20,000 multiple alignments in total).

Phylogenetic analysis

Proteins were aligned using the MUSCLE algorithm[54] and neighbour-joint trees were created using MEGA-X (https://www.megasoftware.net/) . Protein sequence accessions are listed in Table S12.

QUANTIFICATION AND STATISTICAL ANALYSIS

The significance of differences was assessed using Student's *t*-test and are shown in the Figures and Figure Legends. Significance levels were set at p = 0.05 unless otherwise stated. Graphs were plotted using Excel. Error bars are standard error. No methods were used to determine whether the data met assumptions of the statistical approach.